SAND78-7022 [redacted]

LINEAR CONCENTRATING SOLAR COLLECTOR
IN AN AIR-SUPPORTED ENCLOSURE
PRELIMINARY DESIGN STUDY

FINAL REPORT

J. H. Laakso, Project Engineer

D. K. Zimmerman, Project Manager

Prepared For:

Sandia Laboratories
Albuquerque, New Mexico 87115
Project Manager: J. W. McDowell

Contract No. 05-6181

March, 1979

Boeing Engineering and Construction
P. O. Box 3707
Seattle, Washington 98124

Issued by Sandia Laboratories, operated for the United States Department of Energy by Sandia Corporation

---

NOTICE

Printed in the United States of America

Available from
National Technical Information Service
U.S. Department of Commerce
5285 Port Royal Road
Springfield, VA 22161

Price: Printed Copy $6.00; Microfiche $3.00

Distributed according to Sandia Distribution Directive TID-4500-R66, UC-62

TID-4500-R66, UC-62 (316)

5722 J. F. Banas (10)
8266 E. A. Aas
3141 C. A. Pepmueller (Actg) (5)
3151 W. L. Garner (3)
for DOE/TIC
2323 C. M. Gabriel (2)

ABSTRACT

A preliminary design for a low-cost linear parabolic concentrating solar collector in a pneumatically stabilized cylindrical plastic film enclosure and analyses of its theoretical performance and projected costs are described. Potential applications for the concentrator are in heating fluids to the mid-temperature range for use in industrial process heating. The study objective was to develop an inovative design concept having pneumatically stabilized plastic film enclosure as an approach to achieving low collector cost. Both circular film and rigid parabolic reflector concepts were investigated; the concept fulfilling the study objective has a lightweight aluminum honeycomb sandwich parabolic trough reflector with an aluminized polyester film reflective surface. The reflector panels and a black-chrome plated carbon steel absorber tube are supported at intervals by rings with spokes. Cylindrical film enclosure sections are attached to the rings which are supported by rollers; this assembly rotates about the fixed absorber tube and is driven by an electric gear-motor and microprocessor-based control system.

The pneumatically stabilized enclosure provides effective structural rigidity resulting in overall light concentrator weight and good performance in windy conditions. Also, the enclosure completely protects the reflector and absorber from wind, dust and weather. Key design features for a collector with a weatherized polyester enclosure 2.8 m diameter by 30.5 m long (9.33 by 100 ft.) and an aperture area of 69.3m^2 (745.9 ft^2) are given. For this collector configuration, structural analyses, thermal performance modeling, mass-produced component costs, field assembly methods and maintenance requirements are discussed. Daily efficiencies in excess of 45% are predicted with estimated installed field collector costs of \$90/m^2 (\$8.34/ft^2). Results of cost and performance studies indicate that the collector has potential for low cost and offers attractive cost/performance figures-of-merit with further development.

ACKNOWLEDGEMENTS

The support given by Sandia Laboratories' contract technical monitor, Joe McDowell, is greatly appreciated. Thanks are due to the Boeing personnel who contributed to the effort.

Mark Berry	Polymeric Materials Selection
Wayne Davidson	Control System Design
John Laakso	Collector Design/Structural Analysis
William Kaseburg	Production Processes Assembly and Maintenance
Cheryl Warner	Thermal Performance Analysis
John Malcom	Preliminary Performance Modeling
John Schroeder	Collector Design

In addition, the following individual participated in the project:

Larry Johnson — Microelectronics Consultant
Cascade Digital Company
Redmone, Washington

Too numerous to acknowledge are all of the vendors that furnished information for the study. Some of these vendors are listed in the report.

TABLE OF CONTENTS

TABLE OF CONTENTS (Continued)

LIST OF FIGURES

LIST OF FIGURES (Continued)

LIST OF TABLES

1.0 INTRODUCTION

This report describes the preliminary design and the design, performance, and economic analyses of a mid-temperature range, concentrating solar collector. The program was part of a Sandia Laboratories component development project for the design, fabrication, and testing of novel prototype solar energy collectors. The collectors were to be of a modular concentrating design which could operate efficiently in the mid-temperature range (outlet temperature greater than 230°C (446°F)). The primary objective of the Sandia Laboratories project was to stimulate new and innovative collector designs suitable for use in a large field of distributed collectors.

The design concept studied by Boeing Engineering and Construction (BEC) in this program is a lightweight, modular, linear trough solar collector, which employs a cylindrically shaped, transparent plastic enclosure to protect the concentrator surface and the absorber tube. The initial design concept was based on a portion of the cylindrical enclosure (with a reflective metallized film) serving as the concentrator reflective surface, as shown in Figure 1-1. This was potentially a very inexpensive

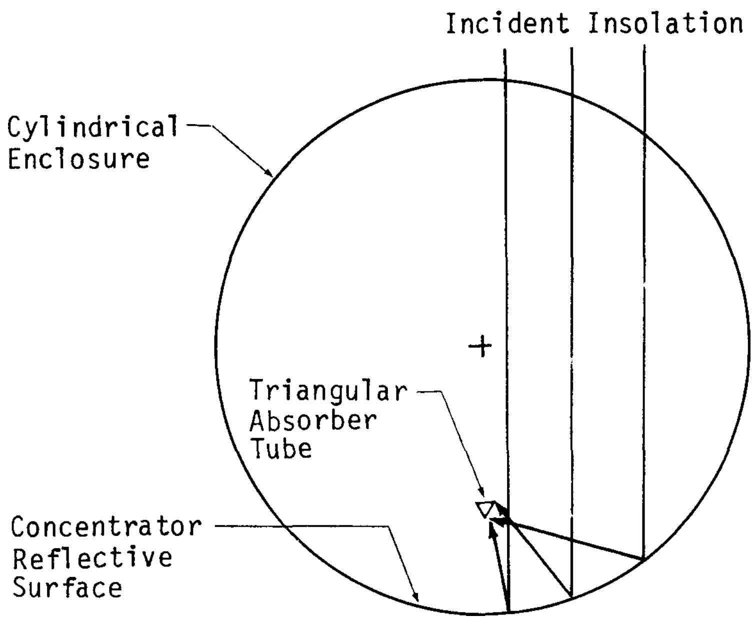

Figure 1-1. Initial Design Concept

construction method, which could lead to reduced cost/performance ratios. Low costs were necessary with this concept because the non-parabolic concentrator shape does not produce a sharp focus, resulting in lower concentration ratios and efficiencies than attained with parabolic concentrators.

The design studies, performance analyses, and production cost estimates on this initial concept led to the following conclusions:

- A relatively large, triangular shaped absorber tube located off the cylindrical axis was required to capture the energy, with the cylindrical concentrator;
- Cost of the triangular absorber tube was higher than anticipated;
- The effective aperture of the concentrator was less than 0.6 times the enclosure diameter;
- Thermal efficiency of the collector was about 40 percent maximum and 36 percent average for the minimum outlet temperature of 230°C (446°F), and decreased rapidly with increasing temperature;
- Performance/cost parameters for the collector were attractive even though the efficiency was relatively low.

The analyses indicated the design concept was acceptable, based on the cost/performance parameters, but suggested that the thermal performance was only marginally acceptable (with a relatively low efficiency) at the required operating temperature. The drop in efficiency at higher temperatures tended to limit the concept usefulness in the mid-temperature range up to about 350°C (662°F). As a result, it was concluded that the concept would be more effective in a lower temperature regime. This application of the inflated cylinder concentrator is being explored by Lawrence Livermore Laboratories (Reference 10).

An alternate concept, similar to one presented in the BEC proposal, was investigated during the remainder of the program. The alternate concept used the cylindrical enclosure as before, but employed a separate parabolic trough concentrator suspended within the enclosure as shown in Figure 1-2. The parabolic concentrator substantially increased the concentration ratio, allowed use of a standard, circular cross section absorber tube on the

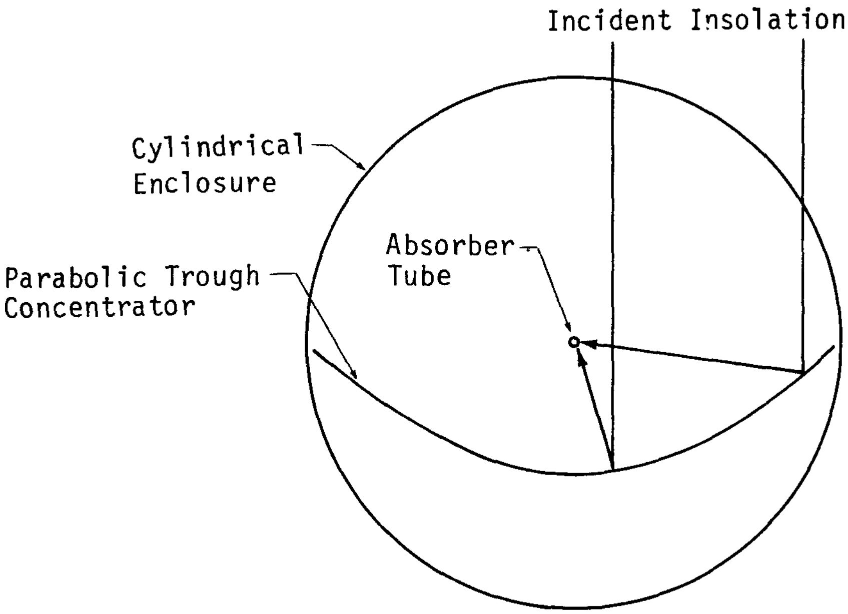

Figure 1-2. Final Design Concept

cylinder axis, and increased the effective aperture to nearly the enclosure cylinder diameter. Description of this concept and its performance forms the bulk of this report.

Section 2 presents a summary of the preliminary design description of the selected, alternate concept. Design requirements for the study are presented in Section 3. Details of the design are described in Section 4. Sections 5 and 6 discuss the design and performance analyses. Concepts for the manufacturing and installation of the collector are given in Section 7, and for maintenance in Section 8. Cost analyses are summarized in Section 9. Conclusions and recommendations are in Section 10.

2.0 COLLECTOR PRELIMINARY DESIGN SUMMARY

This section summarizes the preliminary design and performance characteristics of the selected linear collector, and provides estimated costs for quantity production.

2.1 DESIGN CONCEPT DESCRIPTION

The collector is a linear concentrator which heats a fluid circulated through an absorber tube at the focus. The design concept is a lightweight, modular assembly as illustrated in Figure 2-1. An inflated polyester film enclosure resists environmental loads and supports the internal reflector and absorber tube components. The enclosure also provides stiffness to maintain reflector alignment during sun-tracking rotations. The enclosure film sections are mounted on metal rings that are supported by rollers on wood trusses. The wood trusses are fabricated from treated structural fir and steel truss joint plates similar to conventional home roof trusses.

An aluminum honeycomb parabolic trough concentrator is mounted inside the enclosure as shown in Figure 2-1. The protected environment created by the enclosure permits a very lightweight concentrator design. An aluminized polyester film reflective surface concentrates incoming solar energy onto a tube in which a circulating fluid is heated. The reflector panels have a nominal length equal to the ring spacing less an allowance for differential thermal expansion. Support for the reflector is provided at each ring and at midspan with both fixed and sliding connections.

A carbon steel absorber tube is located at the axis of the enclosure and is supported by a strut and cable structure. A hanger strut connects the reflector and absorber at mid-span to fix the absorber at the focal point. The absorber tube has a black chrome plated surface and an internal concentric hollow pipe plug to improve thermal performance.

Figure 2-1. Collector Installation Concept

A central air system provides filtered dry air to pressurize the collector units. The air requirements are very modest and could be supplied by existing plant air systems through pressure regulators in most cases.

The long axis of the collector unit can be mounted in an East-West or North-South direction, as dictated by the application. Sun tracking is accomplished by rotation of the film enclosure using cables at each ring which are driven by a continuous drive shaft and an electric gear motor. A central control system sends commands to a unit controller at each collector, which adjusts orientation through the drive system. Both the unit and central controllers are based on microprocessor hardware. A digital absolute position encoder on each collector provides angular position data to the closed loop unit control system.

A collector size of 2.8 m dia. by 30.5 m long (9.33 ft by 100 ft) is the baseline configuration for the preliminary design and cost analysis. This size was selected based on the following considerations:

- Available film width for the enclosure.
- Increasing cost effectiveness with module size.
- Shipping limitations on parts and completed collector.
- Absorber tube deflection and stress limitations.

Dimensions are not completely constrained by these factors; the collector configuration could be scaled up or down to suit specific applications.

2.2 PERFORMANCE EVALUATION

Performance predictions for the collector indicate that its efficiency is comparable to other concentrating collector designs. For example, on an average sunny spring day in Albuquerque, with 5 m/s (11 mph) wind, a North-South collector has 47 percent average daily efficiency, total energy output of 3.15 x 10^5 watt-hours, and a water inlet and outlet temperature of 230°C (446°F) and 254°C (490°F), respectively. The water mass flow rate is 0.306 liters/sec (2000 lb/hr).

2.3 COST/PERFORMANCE RATING

After five years of production, yielding a total aperture area of 5 x 10^5 m^2 (5.38 x 10^6 ft^2), the baseline collector is projected to cost \$89.74/m^2 (\$8.34/ft^2) of aperture area (see Section 9.0, Cost Analysis). This cost and the predicted performance based on Albuquerque insolation (see Section 6.0) have been used to obtain the figure of merit defined by Sandia (see definition in Section 3.0) for comparing the collectors. The figure of merit was calculated for each season on both North-South and East-West orientations. The results, which include parasitic power losses, are given below in terms of \$/kJ/day:

COLLECTOR ORIENTATION	FIGURE OF MERIT				
	WINTER	SPRING	SUMMER	FALL	ANNUAL AVERAGE
NS	.04	.0135	.0101	.0139	.0148
EW	.0174	.017	.0157	.0173	.0169

Note that a low figure of merit is desirable. From the tabulation it can be seen that the North-South orientation offers the best annual performance; however, East-West orientation provides significantly better winter performance and is not as seasonally variable as the North-South configuration. For this reason, the East-West orientation might be preferred for those applications where the demand is non-seasonal. A vegetable canner on the other hand might prefer the North-South configuration.

3.0 DESIGN REQUIREMENTS

3.1 SYSTEM APPLICATIONS

The collector is designed to be suitable for large systems utilizing either water or an organic heat transfer fluid (such as Therminol-66) operating near 232°C (450°F). Elements of a water-based system are identified in Figure 3-1. The collector and its controls are designed to operate without direct links to the heat exchanger and fluid flow control system. However, the collector's microprocessor-based control system could be configured to interface with a user's control/data system or to control the overall energy collection and heat exchanger process. The collector is also suitable for both East-West and North-South field orientations.

3.2 REQUIREMENTS AND DEFINITIONS

The general requirements and definitions that governed collector design development are as follows:

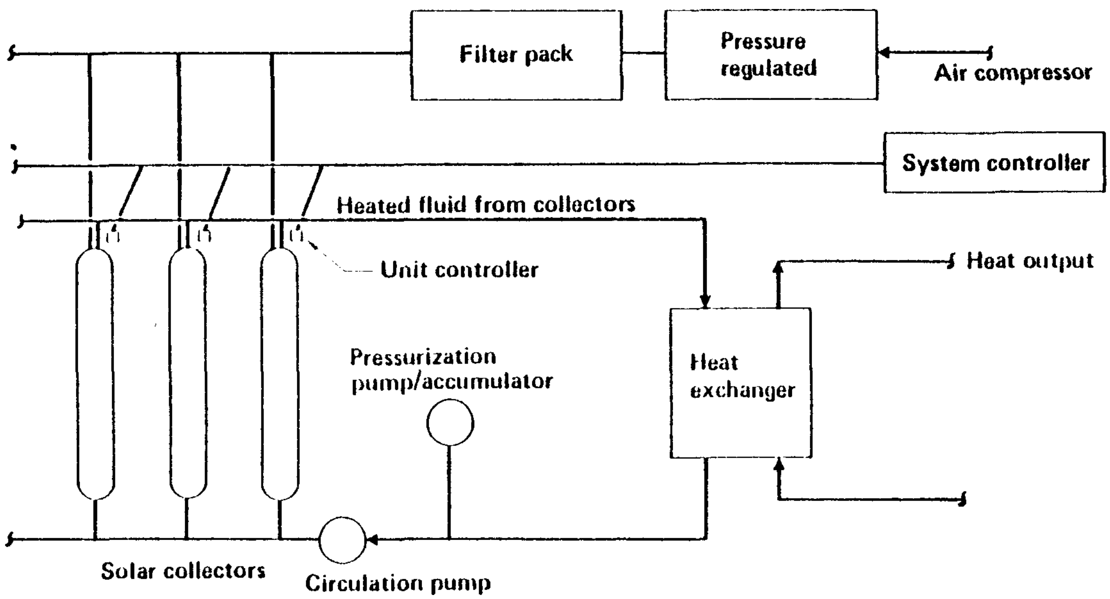

Figure 3-1. System Functional Block Diagram

Solar Collector Module Definition

The solar collector shall be a modular design which consists of a solar radiation concentrator; an absorber; the support structure; and where required, a tracking and drive mechanism. Thermocouples and other instrumentation as required for diagnostic and performance measurement purposes are also a part of the module.

Fluid Requirements

The preferred heat transfer fluid shall be either Therminol-66 or water, although other heat transfer fluids may be used.

Temperature Requirements

The collector shall operate at any outlet temperature above 230^{o}C (446^{o}F).

Pressure Requirements

The maximum allowable working pressure (MAWP) for the collector shall meet or exceed a requirement of 0.51 MPa (75 psig) for Therminol-66. For water the MAWP requirement is a function of the maximum test temperature. At 330^{o}C, the requirement is 12.6 MPa (1860 psig). For lower maximum test temperatures, the MAWP may be reduced to 1.6 times the vapor pressure of saturated steam at that temperature.

Size Requirements

The collector module size shall be suitable for economical mass production for use in a large solar thermal collector field. Test facility limitations dictate flow rates between 0.63 to 63 l/sec (0.1 and 10.0 gpm) and thermal outputs between 1000 kJ/Hr (948 BTU/hr) and 60,000 kJ/Hr (56,900 BTU/hr).

Environmental Requirements

- Wind -- The collectors must be structurally capable of surviving a 40 m/s (90 mph) wind. In addition, the collectors must be capable of operating in a 13 m/s (29 mph) wind.
- Temperature -- The collectors must be capable of operating at ambient temperatures between -30^{o}C (-22^{o}F) and 55^{o}C (131^{o}F).

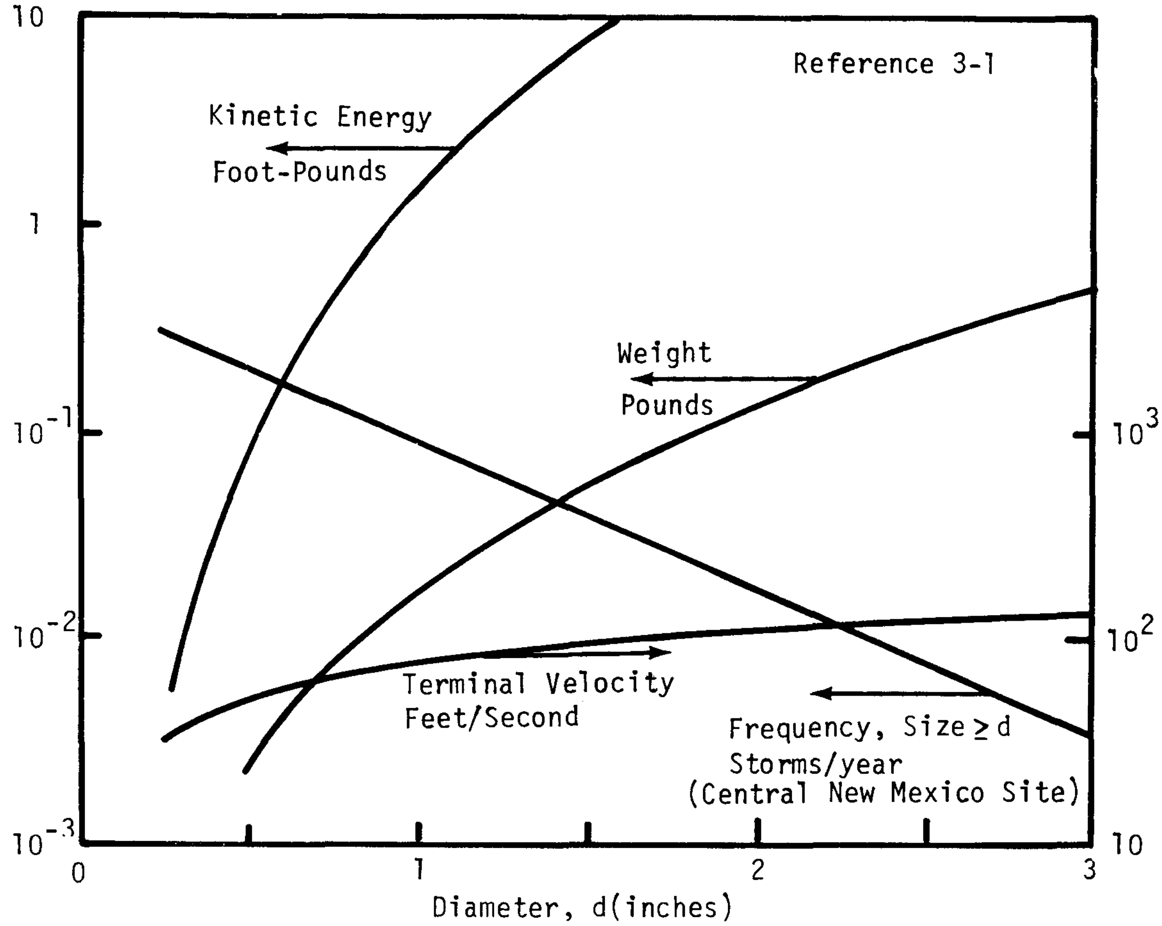

Figure 3-2. Hailstone Environment

- Hail -- Hailstorms can be expected during the design life of the collector. Weight, terminal velocity, kinetic energy, and storm frequency as a function of hailstone size are shown in Figure 3-2 for a site in central New Mexico. The life requirements shall be met cost effectively considering hailstorms.

Life Requirements

A 20 year useful life is required in an outdoor environment. Cleaning, maintenance and repair required to meet the specified life must be addressed, and the cost must be included in calculating operating cost.

General Requirements

Performance analysis shall be based on the following assumptions:

- Average sunny days are assumed. These are defined for each of the four seasons in Section 6.0.
- Assumed temperature data for each of these days are listed in Section 6.0.
- A wind speed of 5 m/sec (11.2 mph) normal to the absorber is assumed for thermal loss calculations.
- Assume that solar noon coincides with clock noon.
- The installation site is located at 35°N latitude and an elevation of 1646 meters (5400 feet) MSL.

Figure of Merit and Efficiency Definitions

The solar collector modules will be rated by a figure of merit which is calculated for each of the four seasons by:

$$M_W = C/(N_c E - B)$$

where: M_W = work figure of merit.

C = total collector construction costs, plus operating costs for 20 years in 1977 dollars, on a mass production basis.

E = thermal energy output per day, kJ/day.

B = electrical energy consumed by auxiliaries per day, kJ/day.

N_c = system cycle efficiency at collector outlet temperature. Use Carnot efficiency, $N_c = 1 - (300/T_{out})$, with T_{out} in Kelvin ($^{\circ}$C + 273).

When calculating collector efficiency, the following definition will be used:

$$\eta = \frac{P_{out}}{P_{in} A}$$

where: η = collector efficiency

P_{out} = power output of the collector as measured by the change in the sensible heat of the working fluid as it passes through the collector, W.

P_{in} = direct normal incident solar radiation, W/m^2.

A = area of the collectors maximum aperture, m^2 (no deduction from area A will be made from the shadow cast by the absorber or associated hardware, i.e., A is a constant).

4.0 DESIGN DESCRIPTION

This section describes the main features of a novel solar energy collector preliminary design. The design is distinguished by an inflated cylindrical enclosure made from a clear plastic film. Contained within the enclosure are a parabolic trough reflector and an absorber tube. The enclosure carries the environmental loads (wind, rain, hail, etc.) so the reflector supports only its own weight. The enclosure provides a calm air space for the absorber tube, eliminating forced convection heat losses. It also protects the reflective surface of the reflector and the plating on the absorber tube from the harsh external environment. The mild environment within the enclosure permits use of less expensive materials and much lighter structure.

Major elements of the design are noted in Figure 4-1, and are discussed in the following subsections.

4.1 ENCLOSURE

The cylindrical and end dome film sections are fabricated from a weatherized polyester film. This type of film is selected because of its high strength, reasonably low cost and current availability. The selected material is Melinex-O polyester film produced by ICI Limited and treated for UV resistance by secondary processing. This film has good optical properties and the UV stabilization offers satisfactory life for prototype collectors.

BEC is currently evaluating a wide variety of clear and aluminized films related to its heliostat program (Ref. 1). In addition, several major film manufacturers are coordinating their proprietary development work on UV resistant films with the BEC program, which may lead to lower film prices and/or improved properties. Table 4-1 shows several candidate films with good performance, although not all of these have long life.

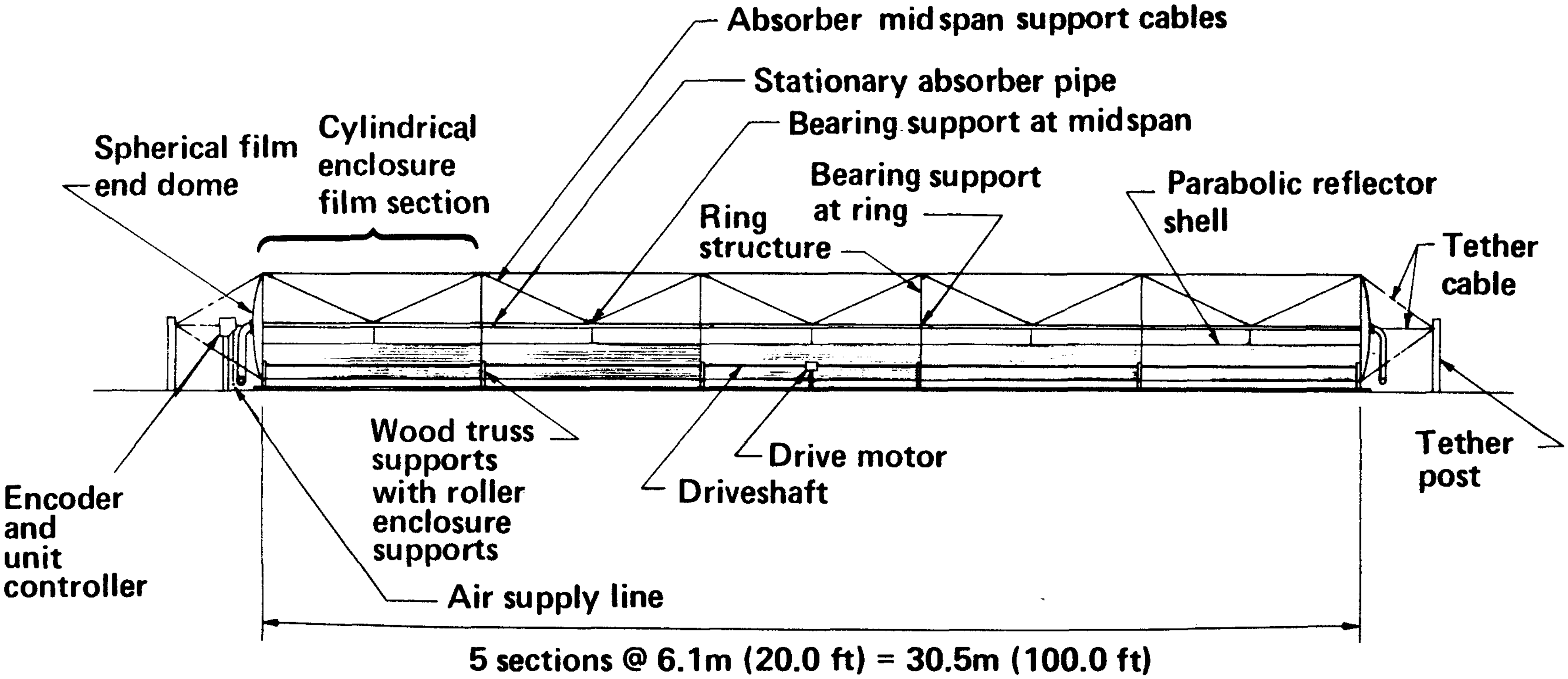

Figure 4-1. Collector System Elements

Due to the lack of real time weatherability data and the inability to correlate accelerated UV test data with real UV life, selected samples are currently installed on racks at the Desert Sunshine Exposure Test Facility near Phoenix, Arizona to receive outdoor exposure. Samples are mounted on south facing racks, tilted at 45° and on sun tracking racks, equipped with multiple mirrors that provide 8 suns exposure.

Table 4-2 shows the loss in optical and mechanical properties for 6 candidates after 6 months on the 45° rack, which most closely simulates real time exposure, and after 6 months accelerated exposure. Examination of the real time data reveals that while polyester may hold up well optically, the degradation in mechanical properties is more severe than the more expensive fluorocarbons. In addition, the fluorocarbons showed little or no property loss in the accelerated exposure testing.

Table 4-1. Initial Mechanical and Optical Properties for Candidate Enclosure Materials

MATERIALS	Ultimate Stress MN/m^2 (PSI)	Yield Stress MN/m^2 (PSI)	Ultimate Elongation %	Specular Transmittance ▷
POLYESTERS				
PETRA A - Non-Weatherable; Allied Chemical	74.5 (10,800)	62.8 (9,100)	544	.89
MELINEX "O" - Weatherable; Martin Process	140 (20,300)	105 (15,200)	90	.84
MELINEX "O" - Weatherable; National Metalizing	185 (26,870)	132 (19,200)	132	.85
POLYESTER - Weatherable; Morton Chemical				.67
POLYESTER - Weatherable; Teijin America				.86
POLYCARBONATE				
POLYCARBONATE - Weatherable; W. R. Grace - 4 MIL	79.9 (11,590)	57.4 (8,320)	141	.88
W. R. Grace - 8 MIL	70.1 (10,170)	56.4 (8,180)	129	.85
POLYPROPYLENE				
POLYPROPYLENE - Non-Weatherable; Hercules	198 (28,740)	44.2 (6,410)	69	.80
Weatherable; Hercules	140 (20,270)	31.0 (4,490)	83	.76
FLUOROCARBONS				
KYNAR - Weatherable Polyvinylidine Fluoride; Pennwalt - KYNAR A	162 (23,520)		80	.89
KYNAR B	167 (24,170)		72	.88
KYNAR C	153 (22,160)		82	.89
TEDLAR - 7826B - Weatherable Polyvinylidine Fluoride; DuPont	78.2 (11,340)	34.5 (5,002)	180	.87

▷ 0.5 cone angle; normal incidence; AM 2 spectrum

Work on polyester stabilization is currently being done by a major film producer (ICI Americas is developing an inherently stabilized polyester film product) and several film post-processors (National Metalizing and Martin Processing). This work potentially will result in a low-cost, long-life polyester film product and BEC has a cooperative program with the vendors to test materials as they become available. Because of the long term nature of this collector development program, low-cost polyester film was selected as the baseline enclosure material, and with continuing film development advances, is assumed to offer a 20 year service life for costing purposes.

Table 4-2. Effect of Solar Exposure on Enclosure Material Properties

	6 month degradation, %							
	Real time (1 sun)				Accelerated (8 suns)			
Material identification	Ultimate strength	Yield strength	Elongation	Spec. trans.	Ultimate strength	Yield strength	Elongation	Spec. trans.
Kynar – Pennwalt	4	0	0	2	6	0	0	2
Tedlar – DuPont	8	4	17	3	13	2	14	6
Melinex-O – Martin Processing	28	17	56	0	72	76	90	39
Polycarbonate – Cryovac	24	10	39	6	25	7	94	52
Polyester – National Metalizing	38	9	86	0	60	100	97	35
Petra A – Allied Chemical	40	85	98	11	100	100	100	24

As shown in Figure 4-2, the cylindrical sections are formed from six longitudinal strips of clear film. Five splices are made in the factory with a heat-set adhesive. The sixth is a field joint consisting of a hook and loop type fastener. A room temperature curing silicone adhesive is supplied to the joint at assembly to increase joint strength and provide positive pressure sealing. The cylindrical section will be shipped rolled up with protective separator paper. The end domes can be fabricated from gore sections; in quantity production, the end domes would be thermoformed. At the edges of the film sections, polyethylene rope will be bonded in place with a wrap-around film doubler to form a bead for attaching to the rings. Bonded doublers will be used in areas of stress such as around the absorber tubes. Sheldahl's thermoplastic adhesive tape for polyester is the selected adhesive system based on considerations of ease of positioning, bonding speed, and wrinkle-free joints.

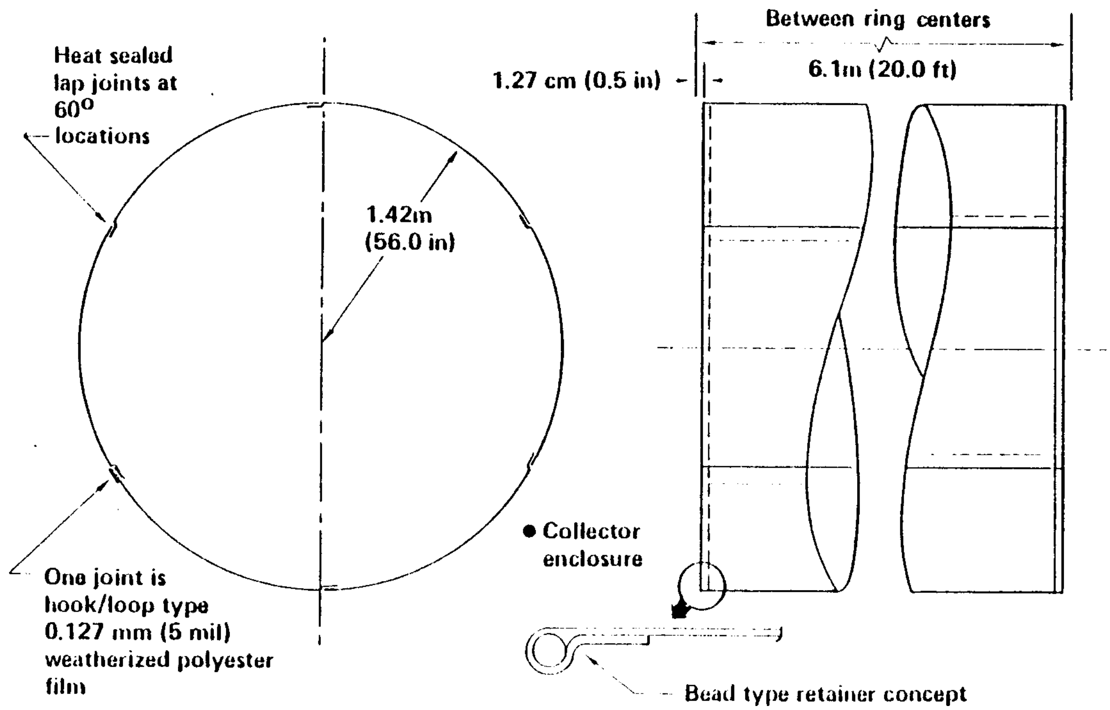

Figure 4-2. Cylindrical Film Enclosure Details

4.2 SUPPORT STRUCTURE

Support structure elements include:

- Rings which provide attachment for the enclosure and for other support structure components.
- Struts and cables from the rings to the reflector and absorber tube.
- Absorber tube bearing assemblies, which permit rotation of the collector about the stationary absorber tube.
- Wood truss bases, that support the collectors with rollers at each ring.
- Cable tethers at each end, which provide backup support for the enclosure when not inflated.

The rings are galvanized steel, roll-framed hat sections. Stiffeners on the lower portion of the ring (Figure 4-3) distribute the film and absorber loads to the support rollers. Attached to each ring stiffener are cables that transmit positioning torque from the drive shaft to the enclosure. Small counterweights at the top of each ring counterbalance the eccentric reflector weight. The cross-section of a ring is shown in Figure 4-4. End beads of the adjacent plastic film sections are positioned on the ring flanges and restrained with band clamps. This ring design allows the cylindrical sections to have convenient lengths for handling and ease of replacement.

The collector design provides for thermal and pressure-induced differential expansion of the absorber tube, enclosure and base. All support rollers are mounted on the trusses with pins that allow the rollers to follow expansion of the enclosure; typical roller details are shown in Figures 4-5 and 4-6. The drive shaft bearings allow the shaft to freely expand. At the end domes, sliding air seals are provided around the absorber and insulation jackets.

Four support struts extend from the ring to support the absorber tube as shown in Figure 4-3. The side and bottom struts in Figure 4-3 also attach to the parabolic reflector, positively positioning it with respect to the absorber tube. Figure 4-7 shows the attachment to the support struts to the ring. The cables which support the absorber tube at mid-span between rings connect to the attachment plates shown in Figure 4-7. The other end of the support struts, Figure 4-8, attach to a bearing mount for the absorber tube. The bearings use ceramic balls to minimize conductive heat loss at the absorber tube supports.

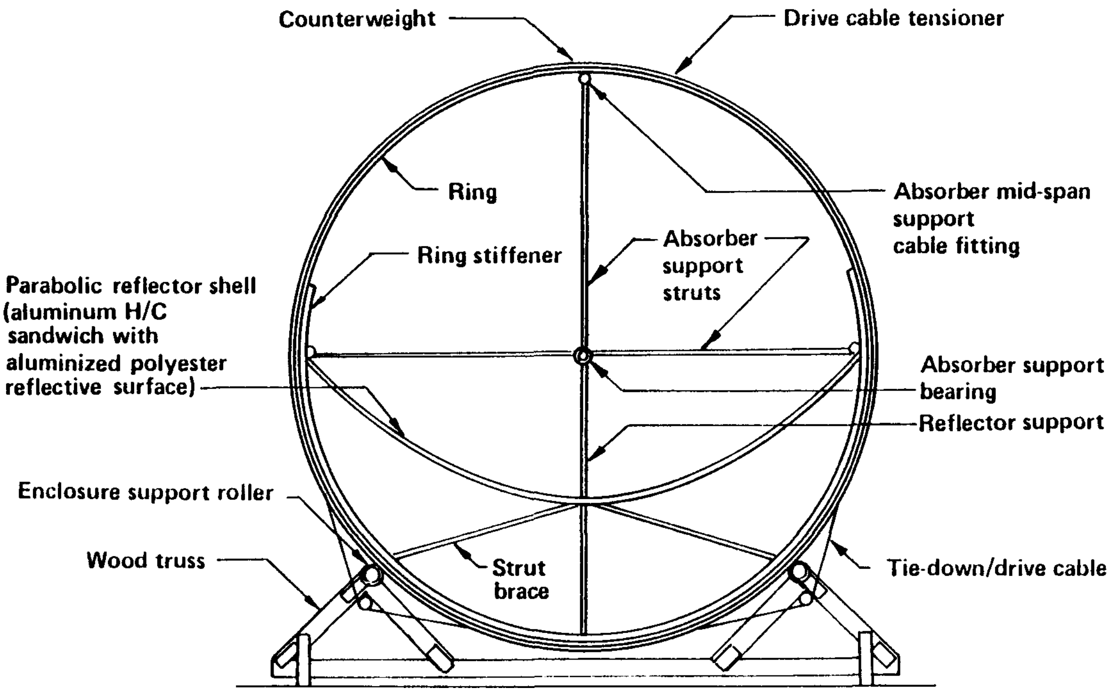

Figure 4-3. Collector Section at Ring Support

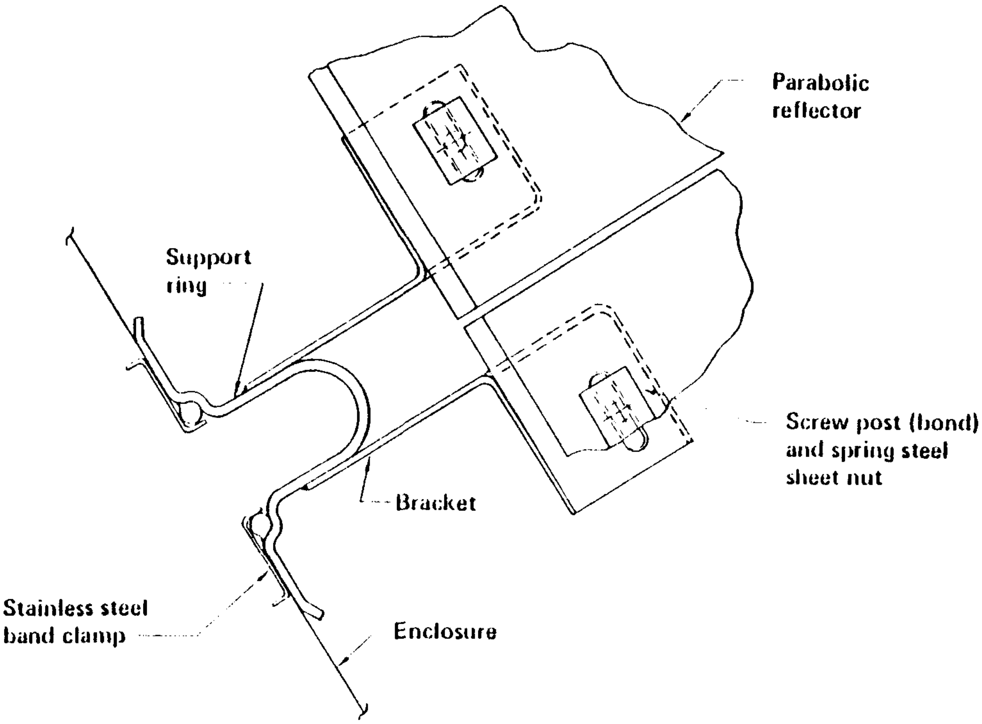

Figure 4-4. Ring Section, Film Clamp, and Reflector Attachment Details

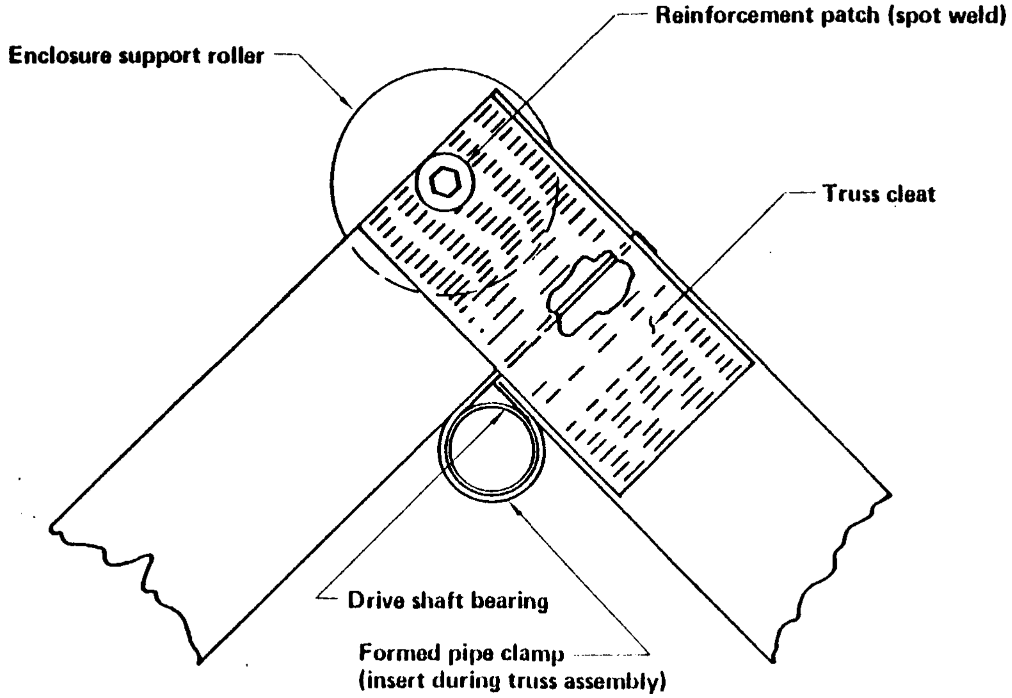

Figure 4-5. Truss Details

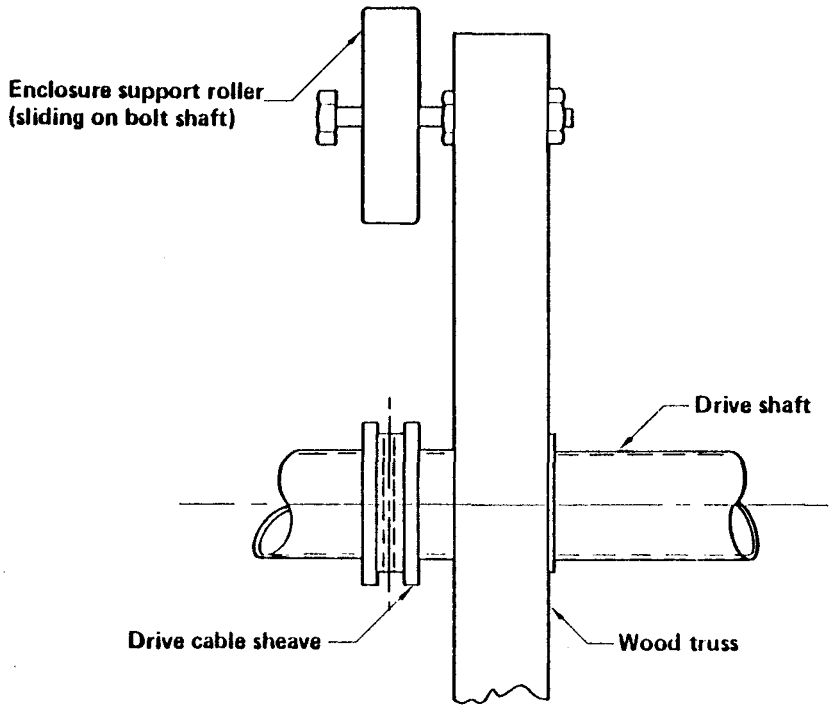

Figure 4-6. Enclosure Support Truss Details

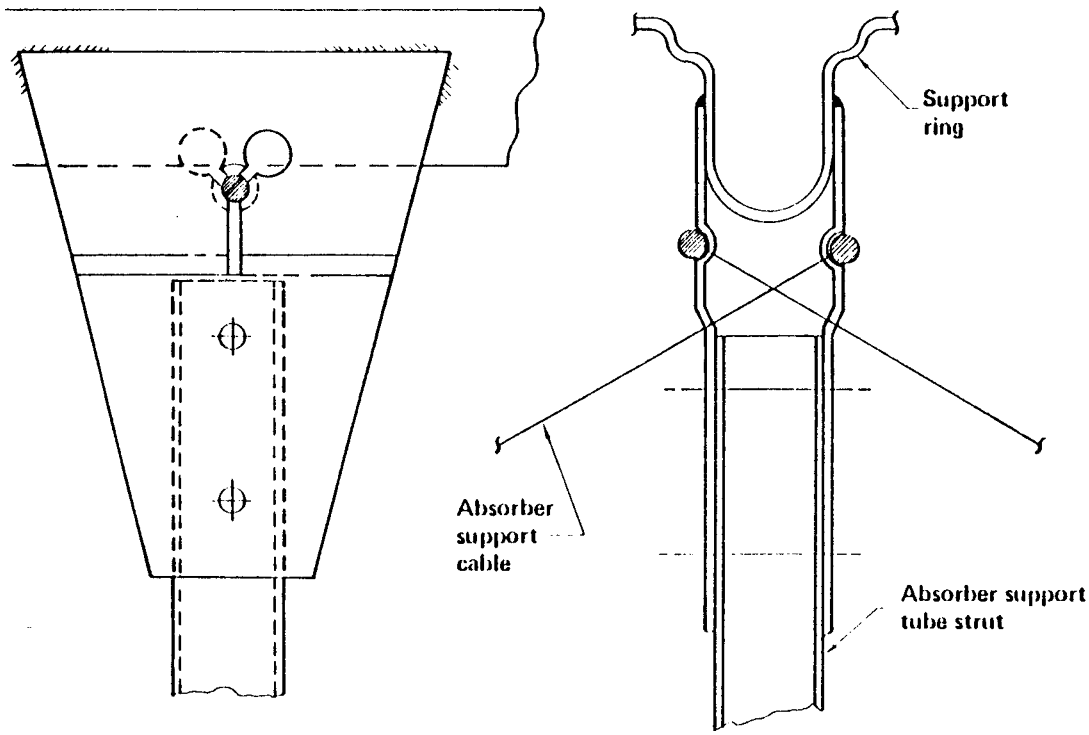

Figure 4-7. Strut-to-Ring Connection Details

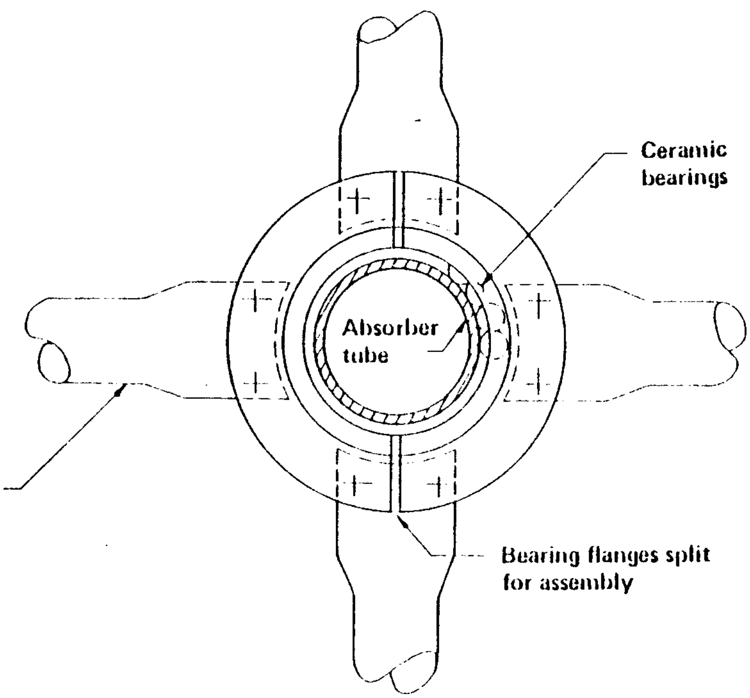

Figure 4-8. Absorber Support Bearing Concept

4.3 REFLECTOR

The reflector is a parabolic shell having a 90^{o} rim angle and focal distance of 0.66 m (26 in). This reflector configuration produces a high energy concentration on the absorber and has the following advantages:

- The effective mirror aperture is a large portion of the enclosure diameter.
- The absorber tube is located on the enclosure axis which significantly reduces the counterweight size and eliminates the requirement for rotary or flexible joints in the fluid loop.
- Reflector structural deflections are lower than for a panel with a smaller ring angle.
- The absorber tube size and cost is minimized because of the good focusing characteristics of the parabolic reflector.
- Enclosure film deflections are uncoupled from the reflector.

The reflector sandwich shell consists of .35 mm (0.014 in) face skins adhesively bonded to 1.27 cm (0.5 in) thick, minimum weight, aluminum honeycomb core in 6 m (20 ft) lengths. The reflective surface is a low-cost aluminized polyester film applied to the aluminum sandwich panels. Because the reflector is shielded from UV radiation and moisture by the enclosure, several aluminized polyester films (shown in Table 4-3, Ref. 1) are suitable for the reflective surface. Hexcell has verified, with test panels, that a satisfactory reflective surface can be obtained on thin 0.014 in face skins. Support points for the shell are provided at the absorber support struts (at each ring) and at the absorber mid-span support points. A clearance of three inches separates the film enclosure and reflector shell to allow air circulation and prevent accidental deflection interference.

Table 4-3. Specular Reflectance for Various Substrate/Coating Combinations

Material	Specular Reflectance (.15° Cone Angle: 633 Nanometer Source)			
	Unstabilized Substrate No Overcoat	Unknown Substrate Overcoated	Stabilized Substrate No Overcoat	Unstabilized Substrate Overcoated
Mylar (Unknown designation - Aluminized (National Metalizing)				.86
Mular D - Aluminized (National Metalizing)	.88			
Mylar D - Aluminized (Dunmore)	.86			
Melinex 442 - Aluminized (Dunmore)	.83			.76
Melinex O - Aluminized (Martin Processing)			.78	
Melinex O - Aluminized (Morton Chemical)	In Test			In Test
Unknown Polyester Substrate (Optical Coating Laboratory)				
Silverized	.88	.84		
Aluminized		.65		

Note: Integrated Air Mass 2 Reflectance Data are expected to be 3% higher

4.4 ABSORBER TUBE

The absorber tube assembly consists of a black chrome plated pressure pipe and an internal hollow pipe plug as shown in Figure 4-9. The pressure pipe section is a 3.175 cm (1.25 in) nominal diameter, Schedule 80, A53 Grade B, carbon steel pipe. This section complies with the ANSI B31.1 Power Piping Code for a span of 3.05 m (10.0 ft) and a maximum allowable working pressure (MAWP) of 18.3 MPa (2650 psig), which corresponds to the MAWP requirements for water at 330^{o}C (626^{o}F).

Forced convection heat transfer coefficients inside the pipe are increased by utilizing a "plug" (a smaller diameter hollow tube inside the pressure pipe) to decrease the hydraulic diameter. For constant fluid temperature, a small hydraulic diameter allows a lower pipe temperature to transfer the same amount of heat into the working fluid, which reduces the radiation and convection losses but increases the fluid velocity and pressure loss.

Figure 4-10 shows the collector end closure including the controller location (see Section 4.4). Figure 4-11 shows the sliding pneumatic seal around the absorber. This seal allows the enclosure to rotate about the fixed absorber with a minimum leakage of air.

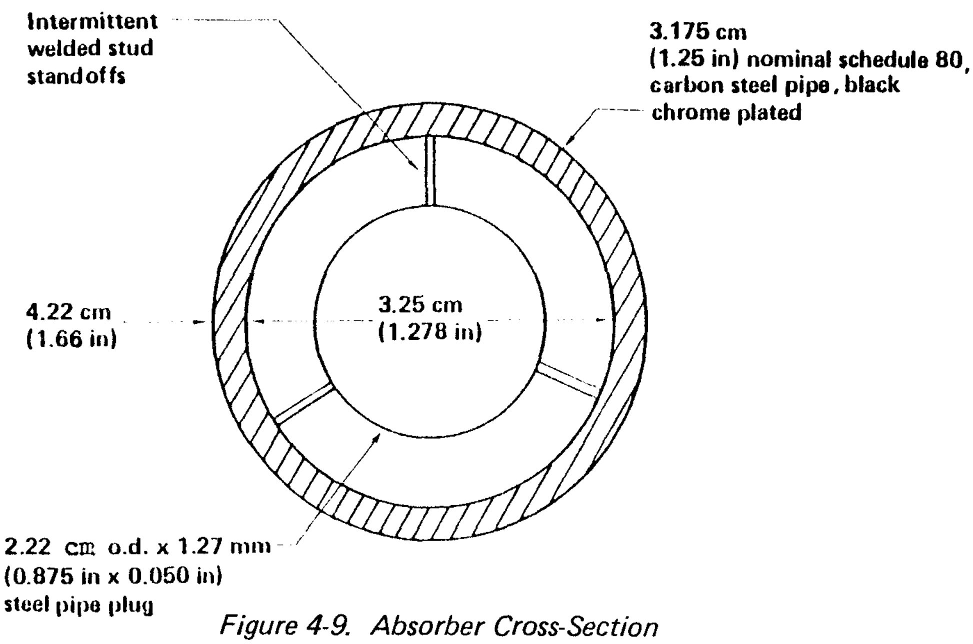

Figure 4-9. Absorber Cross-Section

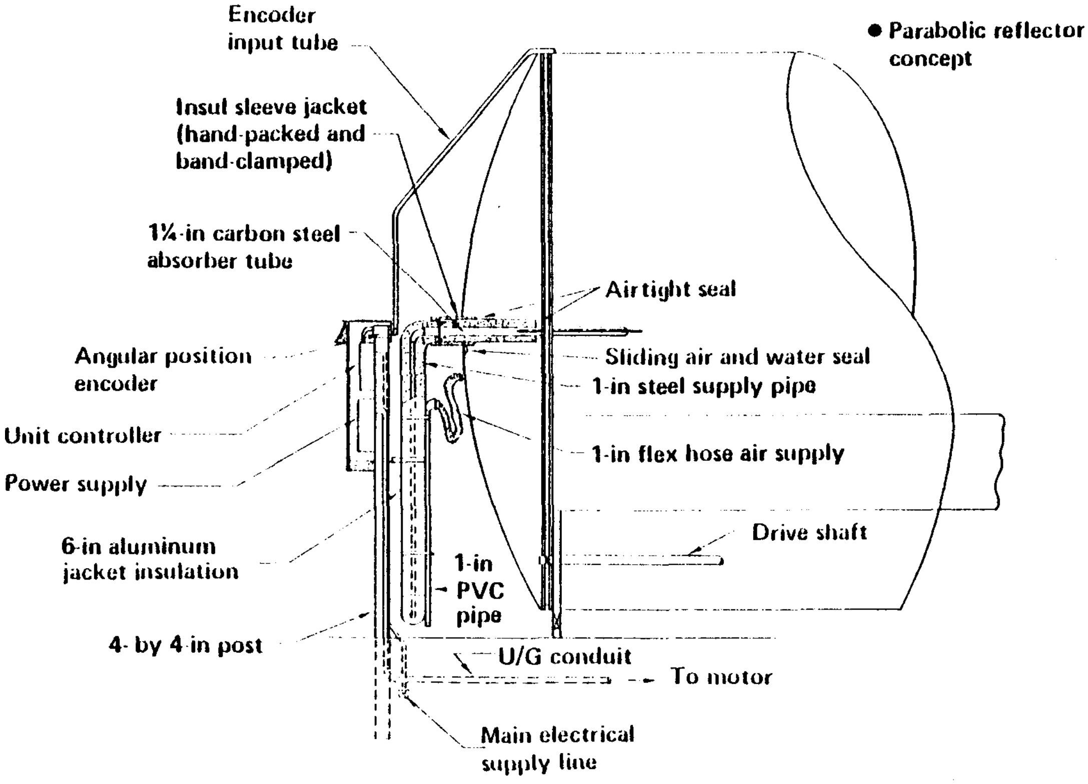

Figure 4-10. Collector End Components

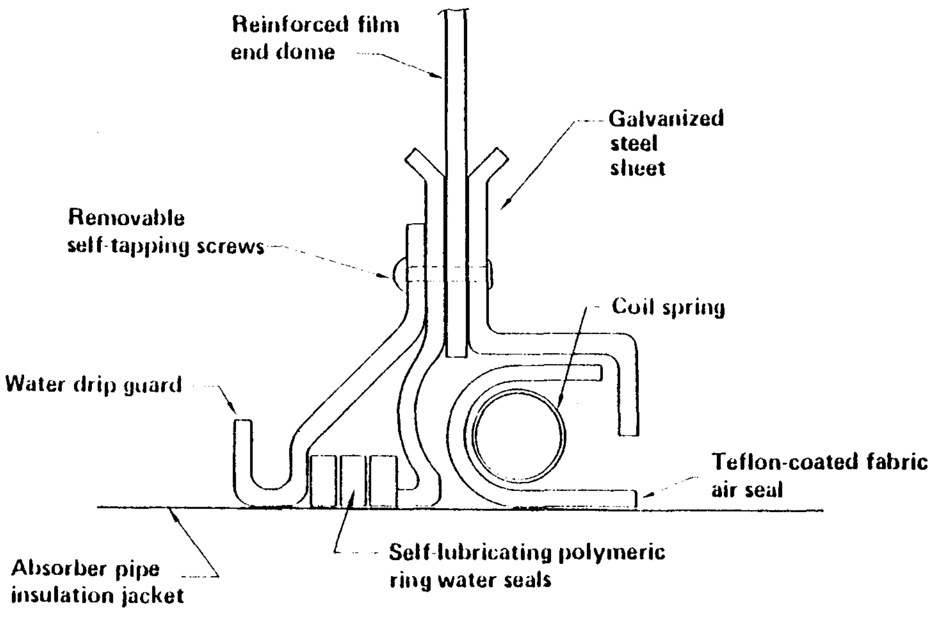

Figure 4-11. End Dome Sliding Seal Concept

4.5 CONTROL SYSTEM

The control system concept selected for the collector is based on microprocessor technology. This fast moving field has evolved to the extent that microprocessor based controls, which were too expensive a few years ago, are now well suited for collector systems. A microprocessor based controller can provide not only a sun tracking capability, but expansion to controlling other components of an energy collection system. Other advantages are:

- Low power consumption.
- Compact packaging.
- Low production cost.
- Easy modification of operational parameters and system expansion.
- Simple interfacing with a data acquisition system.

In a typical installation, the control system's primary functions are to:

- Position the collectors towards the sun.
- Reposition the collectors and sound warnings in case of failure.
- Control the system during start-up.
- Control working fluid flow rate to maintain specified temperatures.

Primary components of the sun tracking control system are identified in Figure 4-12; they are the system controller, unit controller, and interconnecting party line serial data bus.

System Controller

The micro-programmable system controller, Figure 4-13, includes a central processing unit (CPU), random access memory (RAM), programmable read only memory (PROM), clock standard, and optional input/output capability for interfacing with a keyboard-printer terminal and a two-way serial data bus. Universal asynchronous receiver transmitters (UART's) may be used for keyboard printer and serial data bus communications in

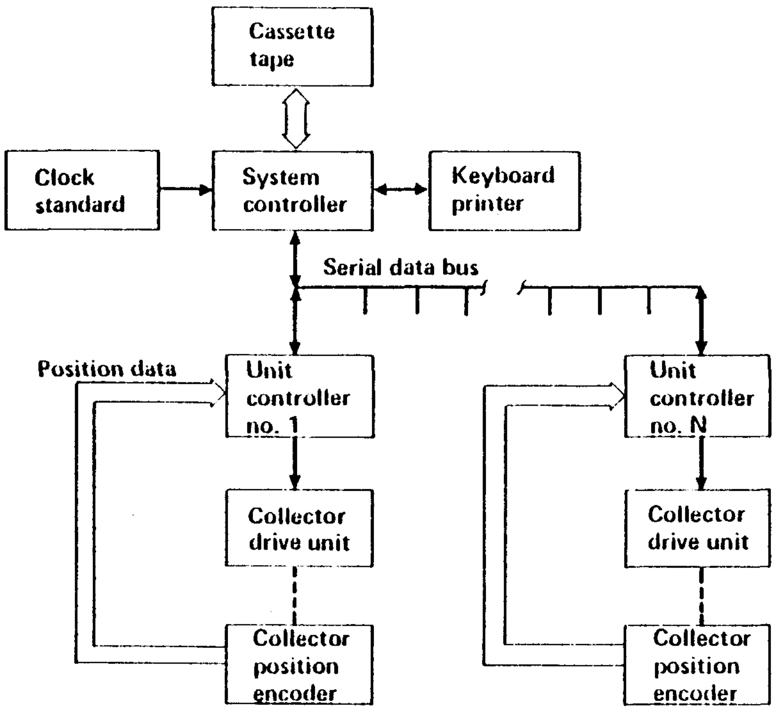

Figure 4-12. Control System Configuration

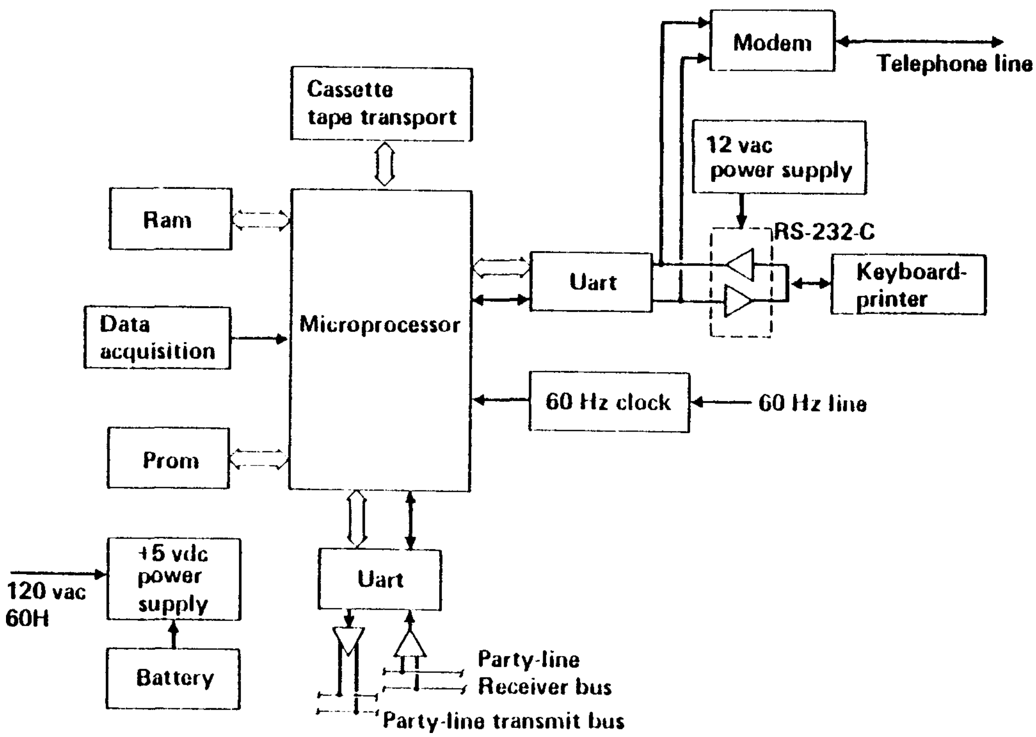

Figure 4-13. System Controller Elements

conjunction with RS-232-C specification and differential voltage driver/receivers. All components of the system controller, with the exception of any RS-232-C driver/receivers, will operate from a single +5VDC power source. This approach provides increased reliability, reduced cost, and a simplified battery backup capability.

The trigonometric calculations required for the proper positioning of each solar collector and the transmission of these data to the respective unit controllers once every thirty seconds is the major computation requirement on the controller. The 30-second update rate maintains a $1/8^{0}$ pointing accuracy for the solar collectors. PROM memory contains the necessary algorithms, instructions, and ephemeris data to calculate tracking parameters for a given day. These are read into RAM memory once each day before tracking begins. In addition, the system controller will have resident firmware which will provide the capability of interactive control from a keyboard pad for checkout and maintenance by an operator. The system controller will also perform critical and routine functions such as fluid temperature evaluation, air pressure monitoring, alarm activation, loss of unit controller communications detection, collector status data processing and storage, and data bus communications control.

Unit Controllers

A unit controller (Figure 4-14) located at each solar collector will contain a micro-computer which will compare true position data from an absolute position encoder mounted on the collector shaft with desired position data as received over the party line communications bus. Appropriate control signals will activate solid-state switches in the motor control power supply unit which will power a fractional horsepower gear motor in a forward or reverse direction, as required to achieve the desired collector position. The above components constitute a closed loop servo system to maintain collector position within the required tracking tolerance.

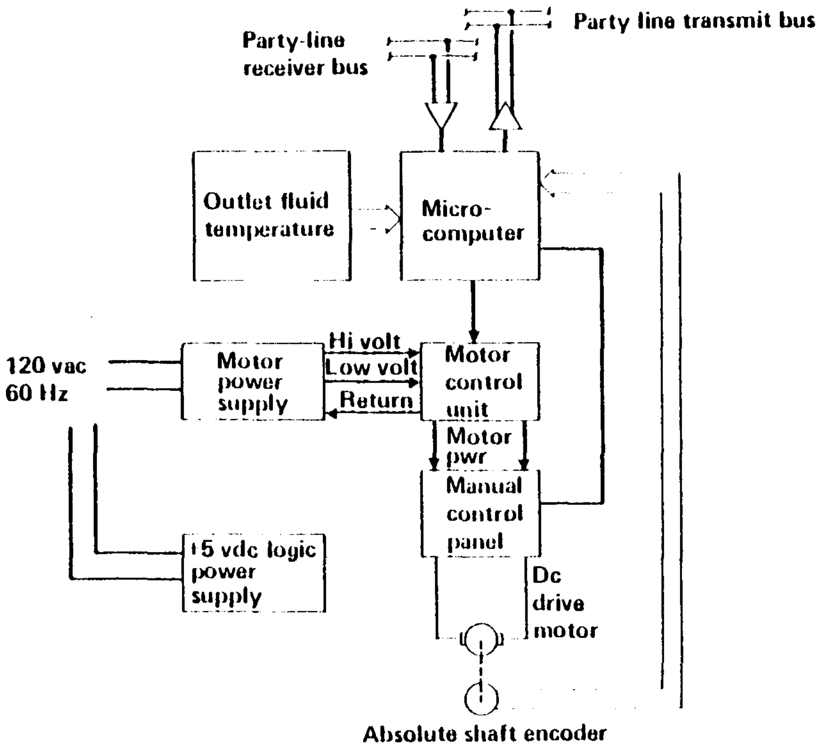

Figure 4-14. Unit Controller

Two motor voltages will be provided:

- A low voltage for normal track mode.
- A high voltage when going to night-time park position and during maintenance operations.

A manual control panel will contain necessary controls to turn off the automatic servo system and allow manual control of the collector drive unit in forward or reverse, high or low speed modes.

4.6 DRIVE SYSTEM

The collector drive system consists of an electric gear motor, continuous drive shaft and drive cables attached to each enclosure ring. A 1/8 horsepower, parallel shaft unit is selected for the gear motor: 300:1 gear ratio Bodine Model 42D3BEPM-E4-175, 100 VDC. This unit has a high gear-reduction ratio which allows a long "on" time increment for increased positioning accuracy. The torque is rated at 35 N·m (310 in/lb) which gives ample reserve torque for overcoming static friction in the support rollers and end dome seals.

The drive shaft is a 5.08 m dia by 0.89 mm wall (2.0 in x 0.035 in) electric resistance welded SAE 1010 steel tube. The tube is sized to minimize wind-up and stresses due to bending. A continuous drive shaft is used so that the collector will rotate in a fail-safe manner in case of enclosure deflation or local damage.

Drive cables are low-cost preformed galvanized steel aircraft cable -- MacWhyte 7 x 19 x 3/32 inch. This cable has adequate flexibility for flexing over the drive shaft and idler sheaves and has a minimum breaking strength of 4450 N (1,000 lb). (The same cable is also used for the collector's tether and absorber support cables.) The cables would be furnished by the factory as assemblies complete with end fittings.

Parasitic power losses for the drive system is estimated to be five watts, assuming a ten percent duty cycle and a North-South collector orientation.

4.7 AIR SUPPLY

Air for collector pressurization is supplied from a central air supply system consisting of a compressor, pressure regulator, filter and dryer units. A rotary vane compressor is a reliable and efficient type of compressor for this application. Several commercial vane-type compressor units are available (for example, GAST manufactures a number of suitable units) that will have extended life because the inflation pressure requirements can be met with low rotational speed. Redundant compressors are planned to provide uninterruptable air supply during vane maintenance and a high reserve flow rate capacity.

Filter/dryer and pressure regulation units would be located downstream of the compressor units; these units would thus have low nominal air flows. The filter units would be assembled from standard catalog items, such as Gelman Type E glass prefilter followed by a Gelman Acropor pore size 0.45 μm filter. Two stage filtering is planned to achieve the air cleanliness requirements as discussed in Section 5.5 (Dust Accumulation Analysis).

In some areas, an air drying unit may be necessary to preclude dew formation inside the enclosure. Experience with heliostat enclosures under life test at Boardman, Oregon indicates that air drying units should not be required. While Boardman is a desert in terms of annual rainfall, 100% relative humidity is encountered frequently during the winter months. If required at a specific site, a number of commercial air drying units are available that could be included in a central air supply station.

The air supply system would supply the collectors with air at a preset inflation pressure level. During periods of steady ambient enclosure air temperature, very low air flow would occur because of the sealed enclosure construction. For sizing purposes, the leak rate was assumed to be 0.006 m^3/min (0.2 cfm) per collector. (Actual leak rates and also air flow management during periods of changing ambient air temperatures will be determined in a detailed design and test program.) Power requirements (parasitic power used in the cost/performance analysis) are expected to be low on a per collector basis. For preliminary design purposes, the air supply power requirement is predicted to be 15 watts per collector for a field of 50 collectors, based on manufacturer's test data (GAST Model 0440 - P103 0.0019 m^3/s (4 cfm) rotary vane compressor) and calculated pressure drop through the filters and distribution lines. Flow sensitive check valves would be located at each collector to prevent system air loss in case of accidental enclosure rupture.

5.0 DESIGN ANALYSIS

5.1 ENVIRONMENTAL LOADS

Wind

A preliminary analysis of wind-induced loads was performed for the lead collector (first row) and mid-field collectors. For the lead collectors, an estimate of local enclosure surface pressures was made for conditions existing behind a porous protective fence such as a chain link wire mesh with intermittent slat inserts. This type of fence is commonly used around industrial facilities and is very effective in reducing downstream wind loading.

Local pressure coefficients are shown in Figure 5-1 for a cylindrical enclosure. These coefficients were obtained by using wind velocity deficits downstream of a protective fence from published test data. Ultimate design upstream wind conditions were assumed to be 21^{o}C (70^{o}F) sea level, and 40 m/s (90 mph) with a 1/7 power velocity profile referenced at 9.1 m (30 ft). Figure 5-2 shows the resultant local pressure distributions on enclosures with various diameters. For a 2.84 m (9.33 ft) diameter, the resultant force vector is upward and has a magnitude of 2100 N/m (144 lb/ft) per unit collector length. At a ring spacing of 6.1 m (20 ft), the total uplift force on the truss foundations will consequently be a low 12800 N (2880 lb) as shown in Figure 5-5 of Section 5.4 (Enclosure Strength Analysis).

For collectors located within a field, wind conditions are relatively calm close to the collector plane. Wind tunnel testing in fields of parallel wires attach to plates (Ref. 9) indicates that local wind-induced pressures at mid-field will be very low and will not govern the design.

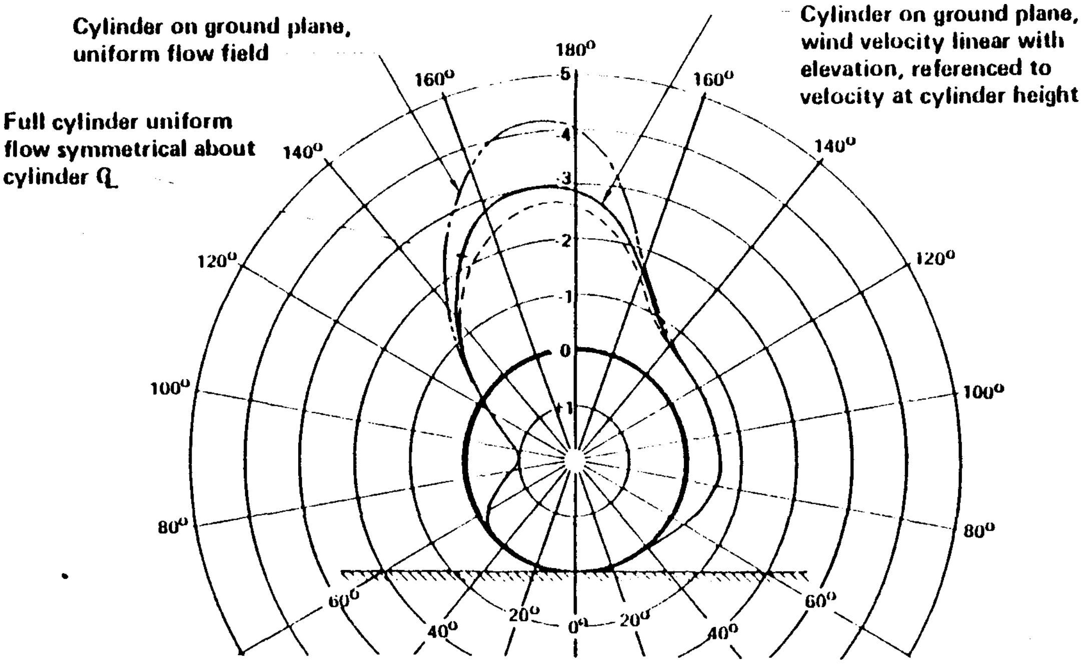

Figure 5-1. Local Pressure Coefficients

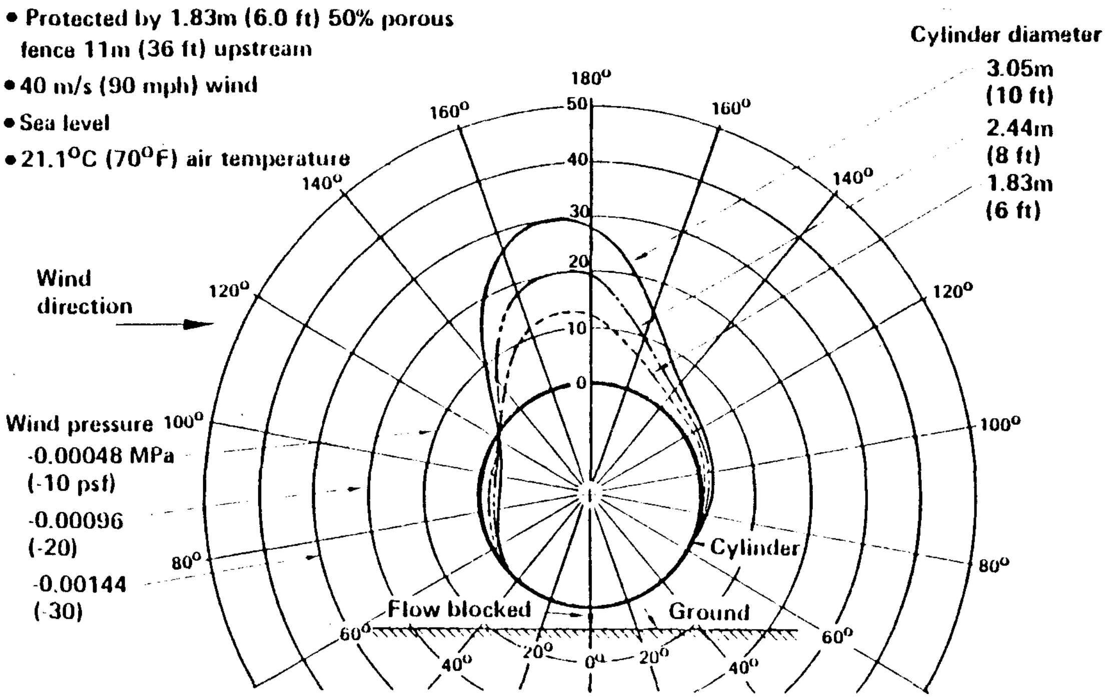

Figure 5-2. Estimated Wind Loads on Outer-Row Collector

5.2 DEFLECTION ANALYSES

A deflection analysis was performed to verify analytically that reflected ray movements on the absorber will be acceptable. Three sources of deflection were analyzed:

- Absorber deflection between supports.
- Enclosure ring, cable and strut deflections.
- Reflector panel deflections.

An ANSYS (Ref. 4) finite element model, illustrated in Figure 5-3, was used to compute general structural deflections. The model has 46 elements having mass and stiffness properties that simulate the "hard" structural components of the collector.

Predictions of deflections due to gravity loads, with the collector in the noon position, are shown in Table 5-1. These preliminary results indicate the structural deflections are small and will not degrade noon-time energy capture. Since the reflector is slaved to the absorber by the support struts, the reflector translational deflection will also be low. For early and late times, however, a detailed incident ray tracing analysis, including sun cone angle effects, will be necessary together with actual testing to verify structural stiffness adequacy.

Local Reflector Deflection

The reflector shell deflection analysis was performed using a finite difference shell analysis code called STAGS-C (Ref. 3). The STAGS-C model and a computer generated contour plot of out-of-plane reflector displacements are shown in Figure 5-4. A special user-furnished sub-routine was prepared for the STAGS-C model involving first and second order partial derivatives of general surface coordinate functions for the parabolic trough shape. The reflector sandwich membrane and bending stiffnesses were generated using the library stiffness routine for

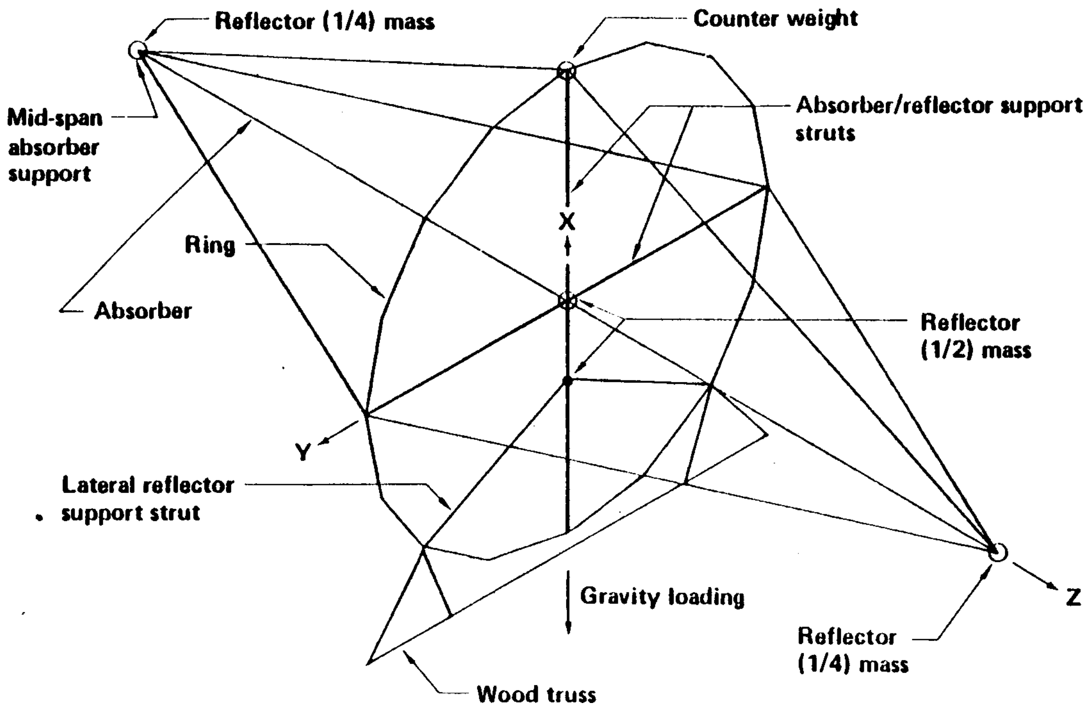

Figure 5-3. Structural Analysis Finite Element Model

Table 5-1. Computed Collector Deflections (ANSYS Model)

ANSYS MODEL NODE LOCATION ALONG VERTICAL CENTERLINE PLANE	DOWNWARD DEFLECTION	
	MM	IN
Counterweight at Top of Ring (0°)	0.169	0.00665
Ring/Strut Connection at Bottom (180°)	0.118	0.00465
Reflector/Strut Connection at 180°	0.127	0.00499
Absorber at Ring Support	0.144	0.00566
Absorber at Mid-Span Support	3.28	0.129
Center of Wood Truss	0.089	0.0035

1 g Gravity Loading at Noon Position

Ansys Model Mass (Weight) 151.2 Kg (333.4 lb)

Reflector Panel Stiffness Not Modeled

sandwich construction. The gravity loading condition in the noon position was simulated by application of a surface normal pressure equal to the reflector sandwich weight: 0.034 kPa (0.005 lb/in^2). The shell point support and symmetry conditions assumed are shown in Figure 5-3.

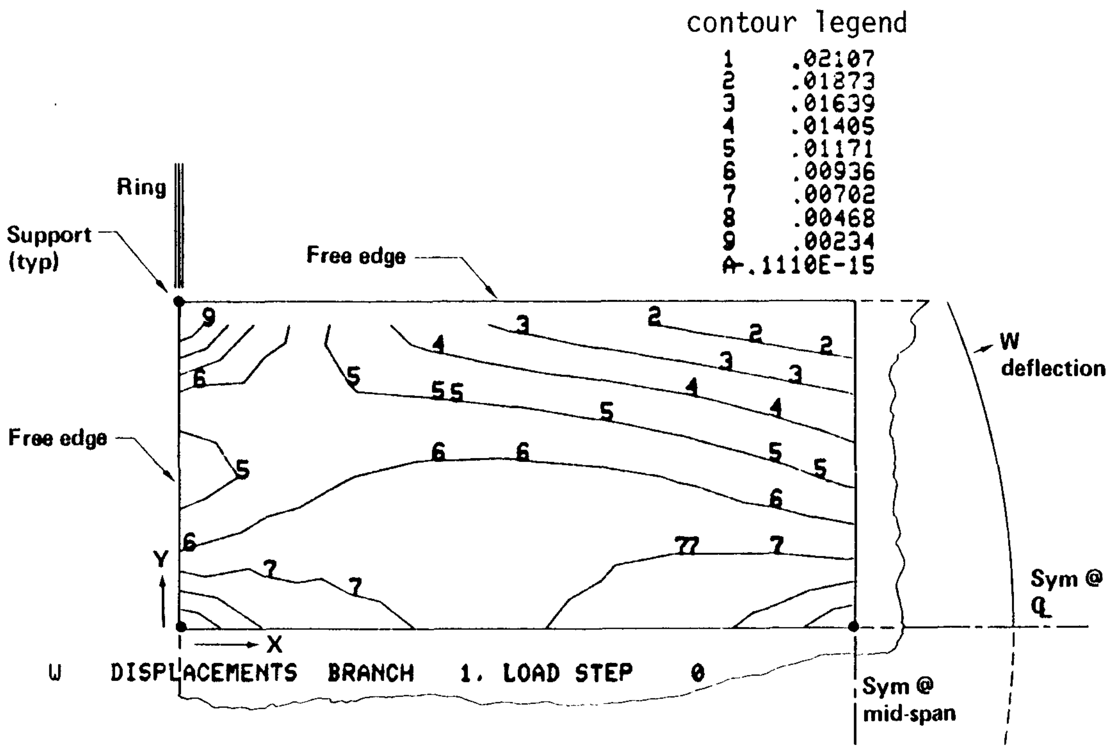

Figure 5-4. Parabolic Reflector STAGS Model

Rays will be deflected most by shell rotations along the free shell edges; results from the STAGS-C model are listed in Table 5-2. The maximum ray intercept on the absorber surface at noon occurred due to rotations at Row 1, Column 5. A shell rotation there of .550 milli-radians corresponds to a ray shift on the absorber of 0.739 mm (0.029 in).

5.3 ABSORBER STRUCTURAL ANALYSIS

A preliminary structural analysis was performed on the absorber pressure pipe; the results are shown in Table 5-3. The pipe section has ample

Table 5-2. STAGS Model Results for Reflector Edge Rotations

EDGE	ROW	COLUMN	ROTATIONS (RADIANS)	
			β_x	β_y
1	1	1	.562E-3	0
1	1	2	-.145E-3	.518E-3
1	1	3	-.239E-3	.934E-4
1	1	4	-.194E-4	-.352E-3
1	1	5	.527E-3	-.549E-3
2	1	5	.527E-3	-.549E-3
2	2	5	.425E-3	-.946E-4
2	3	5	.250E-3	.152E-3
2	4	5	.141E-3	.278E-3
2	5	5	.914E-4	.338E-3
2	6	5	.743E-4	.364E-3
2	7	5	.695E-4	.369E-3
2	8	5	.624E-4	.360E-3
2	9	5	0	.363E-3

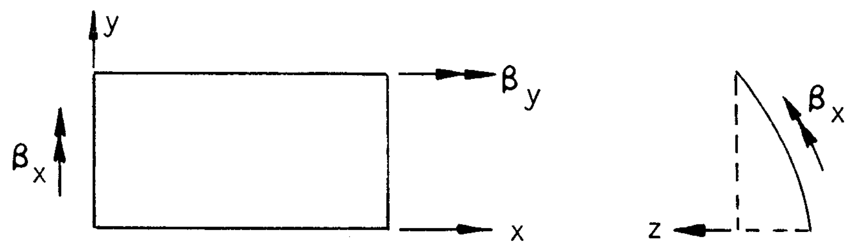

Table 5-3. Absorber Structural Analysis Results

Pressure Pipe Section:	3.18 cm (1.25 in) Nominal Schedule 80 Carbon Steel (A53 Grade B)
Span:	3.05 m (10.0 FT) with Fixed Supports
Weight/Unit Length:	7.13 kg/m (4.79 lb/FT) Including Plug and Water
Maximum Bending Stress:	11.3 mpa (1,642 psi)
Maximum Deflection:	0.86 mm (0.0338 in)
First Bending Mode Frequency:	4.22 HZ

safety margin per the ANSI B31.1 - 1977 Power Piping Code and has low deflections for a maximum operating temperature of 316°C (600°F). Actually, the maximum operating temperature is limited by the long-term resistance of the black chrome plating (Ref. 5). The absorber pipe section has ample strength for dynamic handling and earthquake load conditions. The intermediate absorber couplings are located at the moment inflection points in order to avoid stress concentrations in the seal-welds.

5.4 ENCLOSURE STRENGTH ANALYSIS

The principal loads that the enclosure is subjected to are shown in Figure 5-5. These loads were derived from the wind load data given in Section 5.1 (Environmental Loads).

The enclosure responds to the wind and gravity loads as a continuous beam with the shear load distributed to the rings by film (membrane) shear loads. The internal pressure and the resultant film tension load field are sufficient to preclude shear buckling of the film. Also, the beam-type compressive film loads components are less than the pressure-induced longitudinal tension loads, so film buckling will not develop.

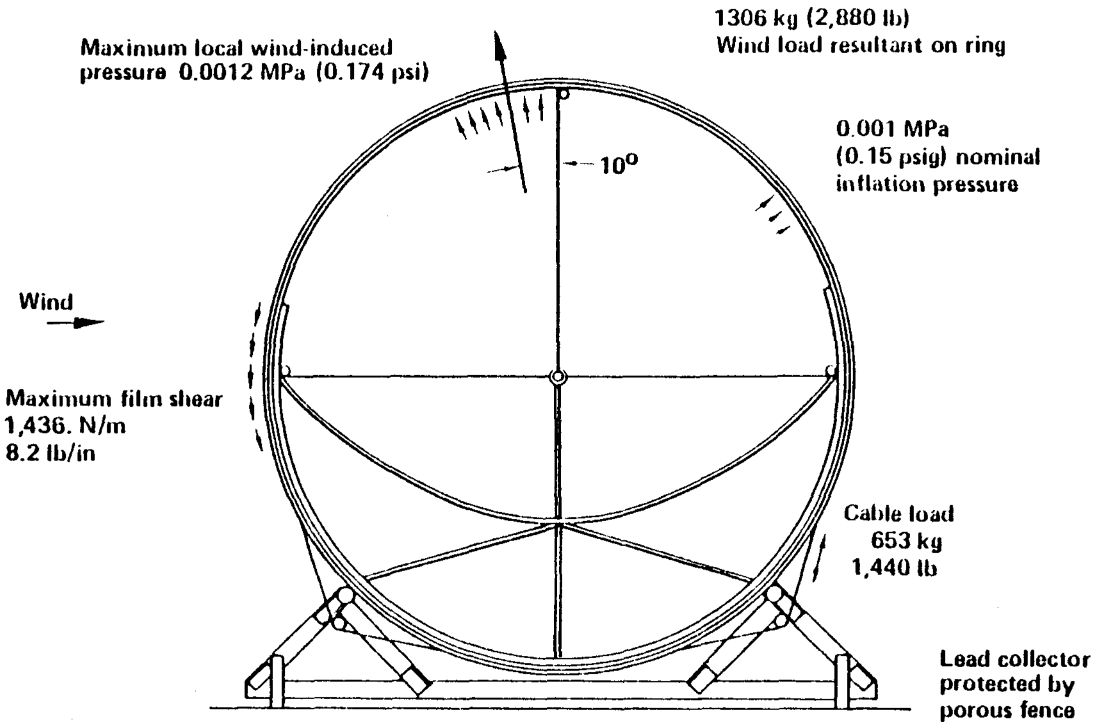

Figure 5-5. Enclosure Design Load Conditions

Local combined pressure loading (inflation static plus wind-induced pressures), produce a maximum film tension stress of 21.1 MPa (3064 psi). The yield stress for Melinex-O polyester film is 103.4 MPa (15,000 psi) so the enclosure is conservatively designed for the ultimate wind conditions. Tests of lap joints having thermoplastic adhesive (Ref. 1) indicate that the film bead and lap joints will be stronger than the nominal 0.127 mm (0.005 in) film.

For a steady-state inflation pressure of 1.03 kPa (0.15 psig), the enclosure film is stressed to 11.6 MPa (1680 psi). Boeing test data

(Ref. 2) for a polyester film (Mylar) at 60^{0}C (140^{0}F) indicates this stress level will not produce significant long-term creep. The test yield stress if 75.8 MPa (11,000 psi).

The drive cables which restrain the collectors at each ring have low wind-induced tension except for the lead (or edge) collectors in a field. The nominal cable size of 3/32 in will need to be increased to provide sufficient breaking strength for the lead collectors. For these collectors, preformed galvanized aircraft cables with a size of 7 x 19 x 5/32 in and having a maximum breaking strength of 12.5 kN (2800 lb) will be required.

The ring "hat" section shown in Figure 4-4 having a depth and gage of 7.62 cm by 1.91 mm (3 x 0.075 in) will have ample buckling strength to resist the radial drive cable reactions. In the support truss roller area, this ring section results in a maximum flange stress of 35.6 MPa (3724 psi) for a 1 g gravity loading based from the finite element model discussed in Section 5.2 (Deflection Analysis). Local ring bending stresses due to longitudinal film tension loads (which tend to pry the hat section open) are 75.8 MPa (11,000 psi). These stresses are reasonably low so the cold roll-formed steel ring section appears to be conservatively designed. The ring and strut bracing design would be optimized in a detailed design program.

5.5 DUST ACCUMULATION

Experience with the heliostat program (Ref. 1) provides confidence that any anticipated dust accumulation can be adequately controlled. The heliostat is a solar energy collector utilizing a plastic enclosure to create a similar controlled environment for reflector surfaces. The studies conducted to predict degradation due to light scattering caused by dust for the heliostat can be applied directly to this collector for an evaluation of its expected performance in a similar environment.

The environment selected for the heliostat program was based on two Arizona extremes; the monthly average for Phoenix of 300 g of particulate per cubic meter of air, and the minimum monthly average for the Grand Canyon of 20 g of particulate per cubic meter. A 15 year operational life was assumed but this can be easily extrapolated to the 20 year life requirement. A loss of less than five percent of the original reflector efficiency was the desired design parameter for loss due to dust accumulation in the heliostat program. The five percent loss was based on the reflector efficiency only and not on the total system performance.

By applying the results of the heliostat study to this collector and by evaluating the effects due to differences in design, the amount of degradation that would be expected in a similar environment can be estimated.

The heliostat model assumed a flow rate of 0.5 cfm to compensate for the rate of leakage. The reduced seal area in this design is not expected to require more than 0.2 cfm of makeup air per unit. The 15 year air volume to reflector surface ratio for the heliostat is:

$$\frac{\text{Air Volume}}{\text{Reflector Area}} = \frac{10{,}252{,}625 \text{ ft}^3}{706 \text{ ft}^2} = 14{,}522$$

For the collector, the 20 year air volume to reflector surface ratio is:

$$\frac{\text{Air Volume}}{\text{Reflector Area}} = \frac{2{,}102{,}400 \text{ ft}^3}{715 \text{ ft}^2} = 2{,}940$$

The lower ratio indicates that the reflector of the collector will degrade less from an equivalent amount of airborne contaminate. If the ratio of glass fiber pre-filter and membrane filter to makeup air volume is maintained at one square inch per 55,000 cubic feet of makeup air, degradation of the reflector surface should not exceed five percent.

There are three additional surfaces upon which accumulation of airborne contaminants would have detrimental effects. The outside surface of the absorber, the inside surface of the collector envelope, and the outside surface of the collector envelope.

The deposition mechanisms acting on the surface of the absorber include diffusiophoresis and photophoresis. Gravitational forces and thermophoresis tend to protect the surface from particulate accumulation. Electrostatic forces are not significant due to the conductive nature of the absorber material. Gravity will protect the surface from particles larger than one micrometer. The force toward the surface for particles less than one micrometer will be the result of the following equation:

$$F_{total} = F_{diffusion} + F_{photo} - F_{thermal}$$

None of these are large enough to be active over more than a micrometer of air around the absorber and do not represent a serious depositional problem.

The inside of the collector may attract particulate due to static charge but the effect is not significant. The model for the reflector assumed all airborne particulate accumulated on the reflector surface.

The convex surface of the external envelope is exposed to the total airborne particulate loading. The forces which deposit particulate on the surface of this envelope include gravity, wind impaction, and diffusion. The strongest forces holding the particles to the surface are gravitational, capillary, Van der Waal, and electrostatic. Because of the convex shape of the surface and the ability to rotate the envelope gravitational adhesive forces can be neglected. With the relatively low humidities expected in these environments, capillary forces can be neglected. The result is that the surface will accumulate predominantly particles below 60 μm. Any particulate larger than that will be removed by wind or gravity with rotation of the envelope. The particles that remain will accumulate predominantly on the upper surface of the envelope. These particles will be a combination of water soluble and insoluble materials that will have to be removed periodically by washing to maintain high efficiencies. Washing is discussed in Section 8.0.

5.6 WEIGHT ANALYSIS

An analysis of collector components is summarized in Table 5-4. A significant portion of the total weight is attributed to the parabolic reflector panels and counterweights. Reflector weight also influences ring design; reduced reflector weight would reduce the basic ring section weight and ring stiffening and/or brace requirements. A detailed design/analysis program aimed at reflector design optimization, is expected to reduce weights in the reflector, counterweight and ring areas.

Table 5-4. Collector Weight Data

Item	kg/m	lb/ft	Relative weight
Film enclosure	1.41	0.95	0.04
Absorber group	4.85	3.26	0.14
Reflector	13.69	9.20	0.40
Ring group	5.30	3.56	0.16
Strut group	1.01	0.67	0.03
Cable group	0.37	0.25	0.01
Counterweights	3.84	2.58	0.11
Wood truss group	1.38	0.93	0.04
Drive shaft group	1.18	0.79	0.04
Misc details	1.12	0.75	0.03
Total	34.15	22.94	1.00

Weight per unit gross reflector area 12.7 kg/m^2 (2.6 lb/ft^2)

6.0 THERMAL PERFORMANCE ANALYSIS

The performance analysis methods and results are presented in this section. Detailed performance results are shown for the collector, as well as seasonal efficiencies, and work and thermal figures of merit.

6.1 PERFORMANCE ANALYSIS MODEL

A computer thermal performance (CTP) model was developed to analyze the collector by calculating efficiency, power output, and work and thermal figures of merit. The CTP code also provided time varying absorber, fluid, and enclosure ambient temperatures. Heat collected and power consumed by the collector are evaluated at half-hour intervals throughout the day. The absorber is modeled as a bare round pipe with a concentric plug.

The CTP code was designed to allow analysis of collectors oriented either North-South or East-West, with sun tracking by rotation about the collector axis.

Trigonometric functions are used to compute time-varying angle of inclination between the incoming sun rays and focal axis of the parabolic trough reflector. The cosine of the inclination angle is then used with the latitude of 35.60 degrees for Albuquerque, to factor the nominal direct insolation at a given time point. Effects of sun cone angle, specular reflectance, local absorber surface incidence angles, and structural deflections are modeled by calculating the reflected sun disk diameter at the absorber based on an average reflected ray length. When this disk diameter equals the absorber diameter, the insolation is factored to zero. This occurs at an inclination angle of 70 degrees to the collector normal. For lesser diameters, the insolation is assumed to vary in a 1/2 power manner from 1.0 for the minimum disk size (at zero inclination to 0.0 at the maximum disk size.

End blockage is treated by using the inclination angle to compute reduced active collector areas in the end collector sections. Both shadowing at the end toward the sun and lost reflections at the end away from the sun are accounted for by deducting an increment of length from the end absorber sections. This time varying length increment is computed for a given inclination angle and an average reflector-to-focal point distance.

Variations in reflector reflectivity and enclosure transmissivity are also modeled as functions of incidence angle, as shown in Figures 6-1 and 6-2 respectively.

Effective aperture, which includes effects of absorber shadowing, side enclosure-to-reflector gap, enclosure side transmission losses at high local incidence angles, support structure shadowing and optical aberrations due to deflections, is estimated to have a value of 0.8 of the enclosure diameter.

The time varying insolation data used are typical normal direct insolation values for each season for Albuquerque, New Mexico, furnished by Sandia Laboratories. The insolation curves are presented with the calculated efficiency curves in Figures 6-7 to 6-10 in Section 6.2. The ambient temperature profiles used were also furnished by Sandia Laboratories. Values for the typical seasonal temperature profiles are listed in Table 6-1.

The heat transfer fluid can be either water or Therminol-66. The temperature dependent physical properties for both water and Therminol-66 were incorporated into the program for the working temperature range. The properties shown in Table 6-2 are typical physical values at $450^{\circ}F$ for these fluids. Complete information regarding Therminol-66 is available from the Monsanto Company (Ref. 6). Material properties used for the various collector components are shown in Table 6-3. These properties were obtained from Boeing test data (Ref. 1) and vendor literature.

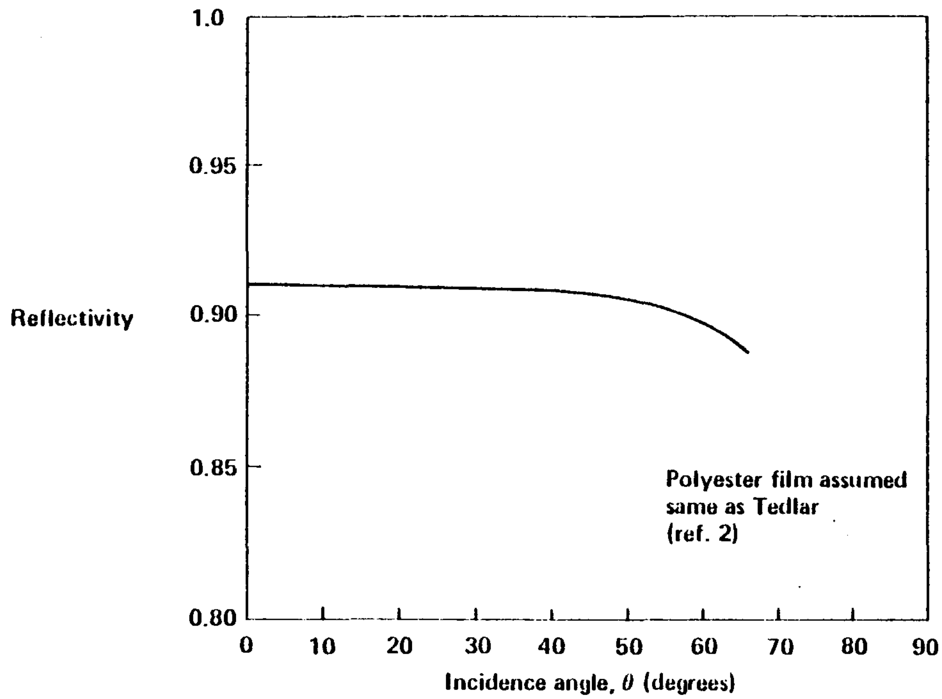

Figure 6-1. Reflectivity Versus Incidence Angle Model

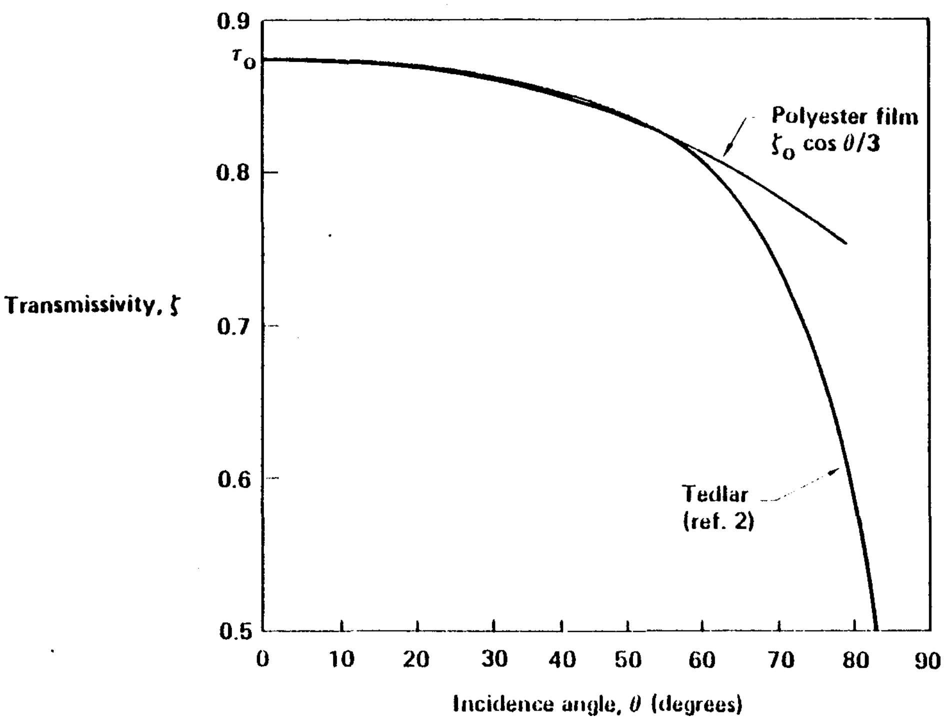

Figure 6-2. Transmissivity Versus Incidence Angle Model

Table 6-1. Typical Temperature Data for the Four Seasons

Hour	Temperature ^{o}C (^{o}F)			
	Winter	Spring	Summer	Fall
Midnight	0.0(32)	5.6(42)	17.8(64)	16.7(62)
1	-1.0(30)	5.0(41)	18.9(66)	16.7(62)
2	-3.3(26)	5.0(41)	17.8(64)	16.1(61)
3	-3.3(26)	5.0(41)	17.8(64)	15.0(59)
4	-3.3(26)	3.9(39)	17.8(64)	15.0(59)
5	-2.2(28)	2.8(37)	15.6(60)	15.0(59)
6	-3.3(26)	2.8(37)	16.7(62)	15.0(59)
7	-3.3(26)	1.7(35)	20.0(68)	15.0(59)
8	-3.3(26)	2.8(37)	21.7(71)	15.6(60)
9	0.0(32)	3.9(39)	25.0(77)	18.9(66)
10	3.9(39)	6.7(44)	26.7(80)	21.7(71)
11	6.7(44)	7.8(46)	28.9(84)	22.8(73)
12	7.8(46)	10.6(51)	31.7(89)	25.6(78)
13	10.0(50)	10.0(50)	33.9(93)	25.6(78)
14	11.1(52)	11.7(53)	33.9(93)	26.7(80)
15	12.8(55)	13.9(57)	32.8(91)	26.7(80)
16	12.2(54)	12.8(55)	32.8(91)	25.0(77)
17	10.0(50)	12.8(55)	32.8(91)	25.0(77)
18	8.9(48)	10.0(50)	32.8(91)	25.0(77)
19	6.7(44)	7.8(46)	32.8(91)	25.0(77)
20	6.7(44)	6.1(43)	30.0(86)	23.9(75)
21	6.7(44)	3.9(39)	27.8(82)	21.7(71)
22	7.8(46)	2.8(37)	25.0(77)	21.7(71)
23	6.7(44)	2.8(37)	23.9(75)	20.0(68)
Midnight	6.7(44)	1.7(35)	21.7(71)	20.0(68)

Table 6-2. Typical Working Fluid Properties at 450^{o}F

Property	Therminol-66	Water
Thermal Conductivity k, Btu/hr-ft-°F	.0596	.3675
Viscosity, μ, lb/sec-ft	45.8×10^{-5}	7.73×10^{-5}
Density, ρ, lb/ft^3	58.3	51.5
Specific Heat, c_p, Btu/lbm°F	0.558	1.12

Table 6-3. Material Properties Used in Performance Analysis

• Enclosure (weatherized polyester film)	
Solar absorptance	**0.03**
Solar transmittance	**0.87**
IR transmittance	**0.20**
IR emittance	**0.80**
• Receiver (black chrome plated steel)	
Solar absorptance	**0.92**
IR emittance	**0.1**
• Reflector (aluminized polyester)	
Solar reflectance	**0.88**

An energy balance on the collector is shown in Figure 6-3. The following heat flows are modeled in the CTP code.

Q_1 = Direct normal solar radiation on collector.
Q_2 = Diffuse solar radiation on collector.
Q_3 = Direct solar radiation on receiver.
Q_4 = Diffuse solar radiation on receiver.
Q_5 = Radiation between receiver and enclosure.
Q_6 = Convection between receiver and enclosure air.
Q_7 = Convection between enclosure and enclosure air.
Q_8 = Convection between enclosure and ground.
Q_9 = Convection between enclosure and ambient air.
Q_{10} = Convection between receiver and fluid.
Q_{11} = Radiation between receiver and sky.
Q_{12} = Radiation between enclosure and sky.

Temperatures are calculated by an iterative process at a number of sections along the collector (typically 10). Estimated temperatures are used to perform an energy balance on the collector from which the absorber, fluid, and enclosure air temperatures are calculated. If the calculated values and the estimated values agree within $1^{\circ}F$, the program

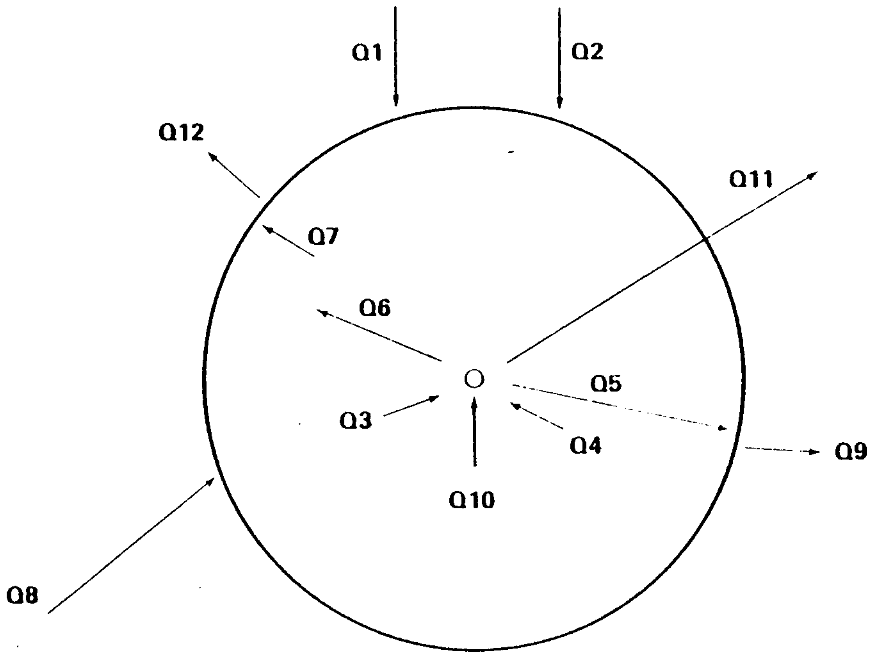

Figure 6-3. Heat Flows in Collector Heat Balance Analysis

proceeds. Otherwise, the calculated values are used for the new estimated values in the energy balance. Temperature evaluation occurs at each section of the collector. Only the initial inlet temperature is specified as an input to the analysis. The program calculates the outlet temperature for the first section, then uses it for the inlet temperature to the second section. After all sectional temperature calculations are complete, the heat gain is evaluated. Using computed fluid pressure loss, calculations are made to determine pumping power losses, and sectional and total collector efficiencies at half-hour intervals having varying insolation and ambient temperature values. Finally, an average daily efficiency, work figure of merit and thermal figure of merit summary parameter are calculated.

6.2 PERFORMANCE PREDICTIONS

Typical performance characteristics of the collector are shown in Figures 6-4 to 6-7. These examples are for a North-South oriented collector with water for the heat transfer fluid, and the summer season. The fluid parameter $(T_f - T_a)/g_i$ in Figure 6-7 is the ratio of the difference between the average fluid temperature and the ambient temperature, and the direct solar flux. Parasitic pumping losses for both heat transfer fluids as a function of flow rate for the spring case are presented in Figure 6-8.

Efficiency of the collector can be examined in three ways: an hourly efficiency versus time, an average seasonal efficiency, and an average efficiency versus a fluid parameter. The hourly efficiency, as defined in Section 3.0, for each season with respect to time is shown in Figures 6-9 to 6-12. Concentrator conditions are noted. These figures also show the insolation profiles for each season. Average seasonal efficiencies are presented in Figure 6-13 for Therminol-66 and water and North-South and East-West orientations. Other collector conditions are noted on the figures.

Power production throughout the day is presented for each season in Figures 6-14 to 6-17. Work and thermal figures of merit values for each season are shown in Figures 6-18 and 6-19. Work figures of merit was defined in Section 3.0. Thermal figure of merit is the ratio of collector cost to net thermal energy into the working fluid. Figure of merit values are based on a reference collector cost of $\$10/ft^2$ ($\$108/m^2$); the values are adjusted for the estimated collector cost in the data given in Section 2.3 (Cost/Performance Rating).

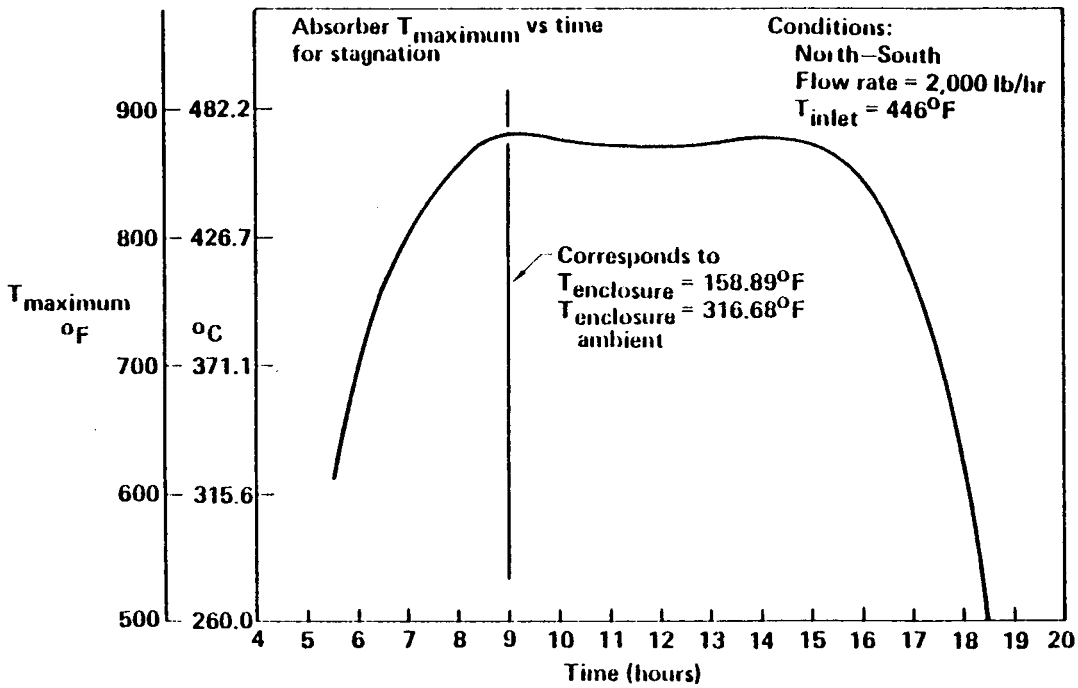

Figure 6-4. Typical Absorber Stagnation Temperatures

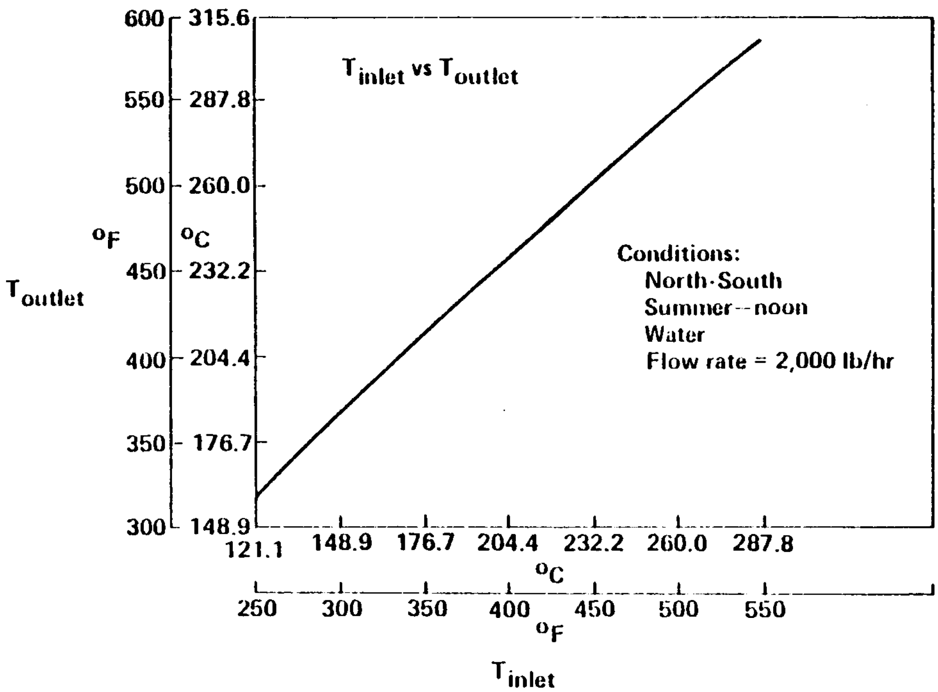

Figure 6-5. Typical Inlet Versus Outlet Temperatures

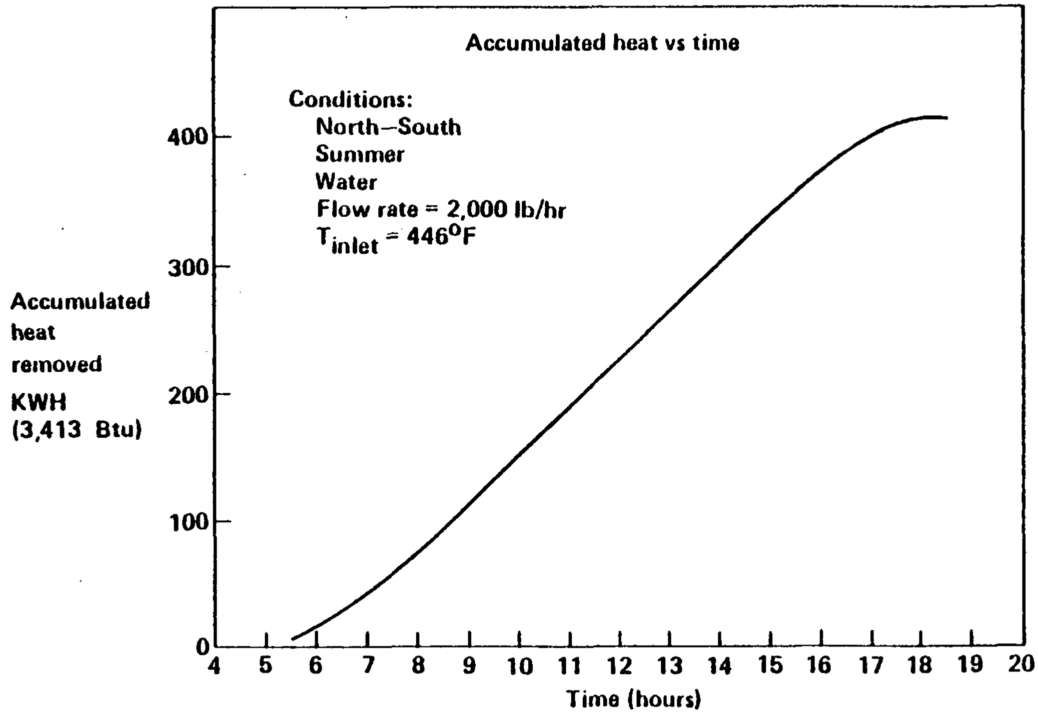

Figure 6-6. Typical Cumulative Heat Collected

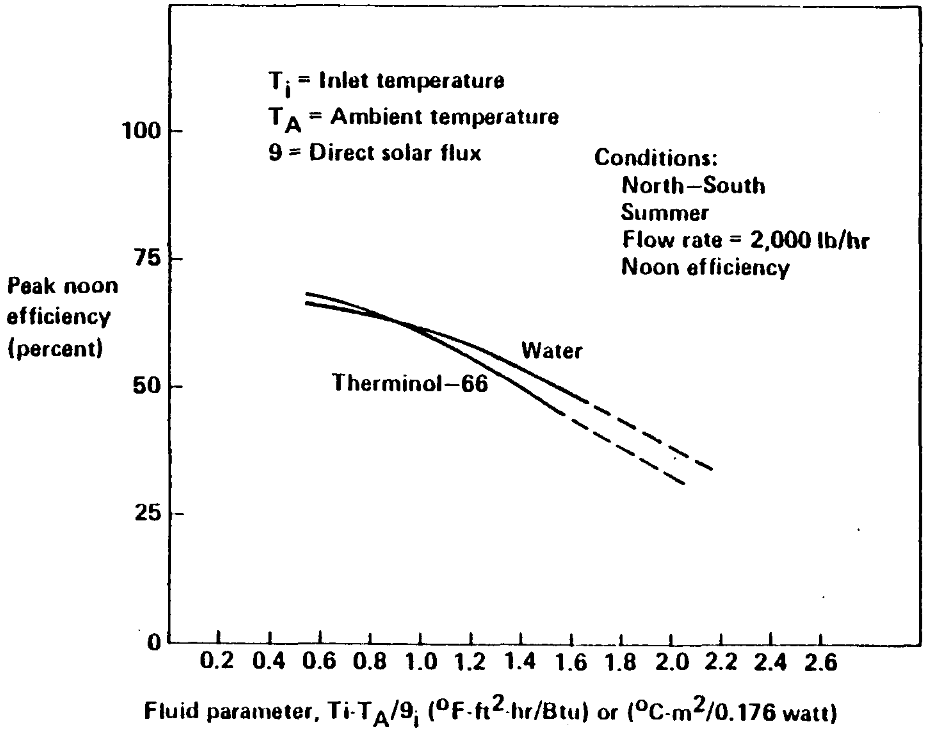

Figure 6-7. Typical Peak Noon Efficiencies

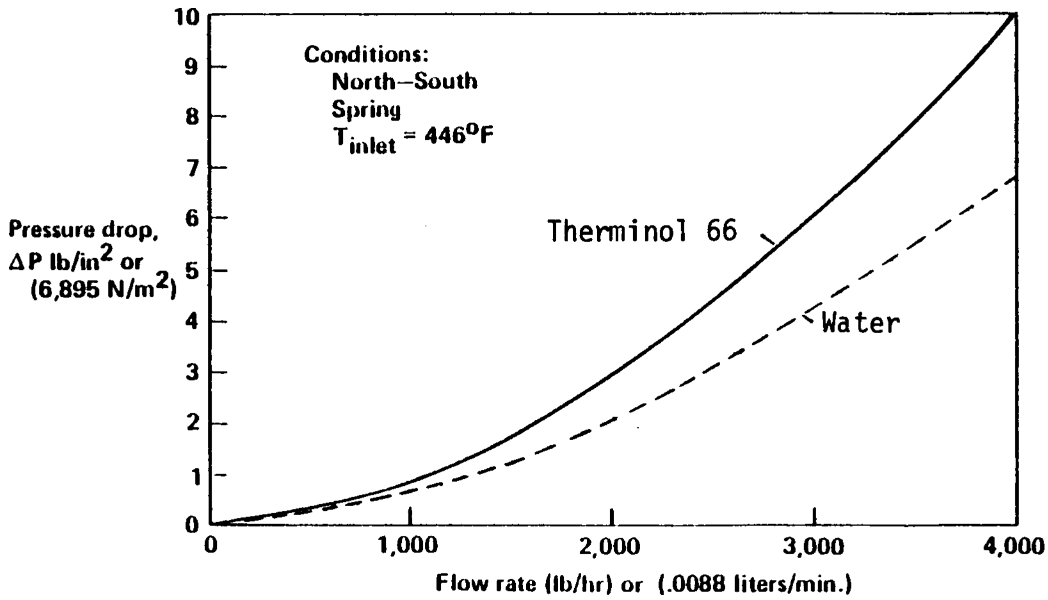

Figure 6-8. Typical Parasitic Pumping Losses

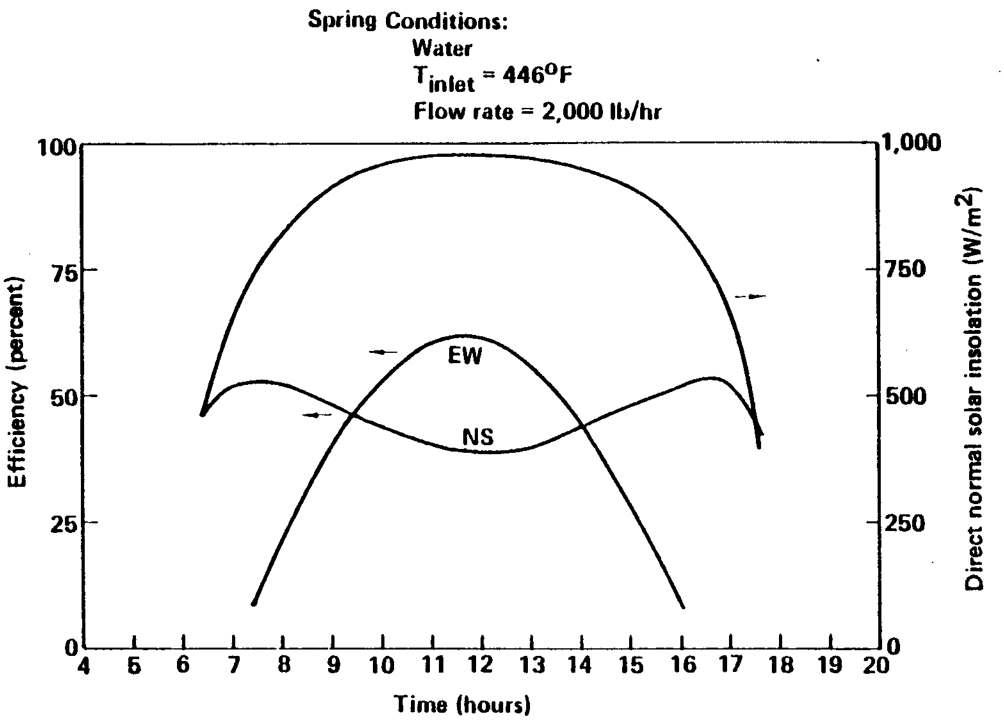

Figure 6-9. Daily Efficiency Profile – Spring

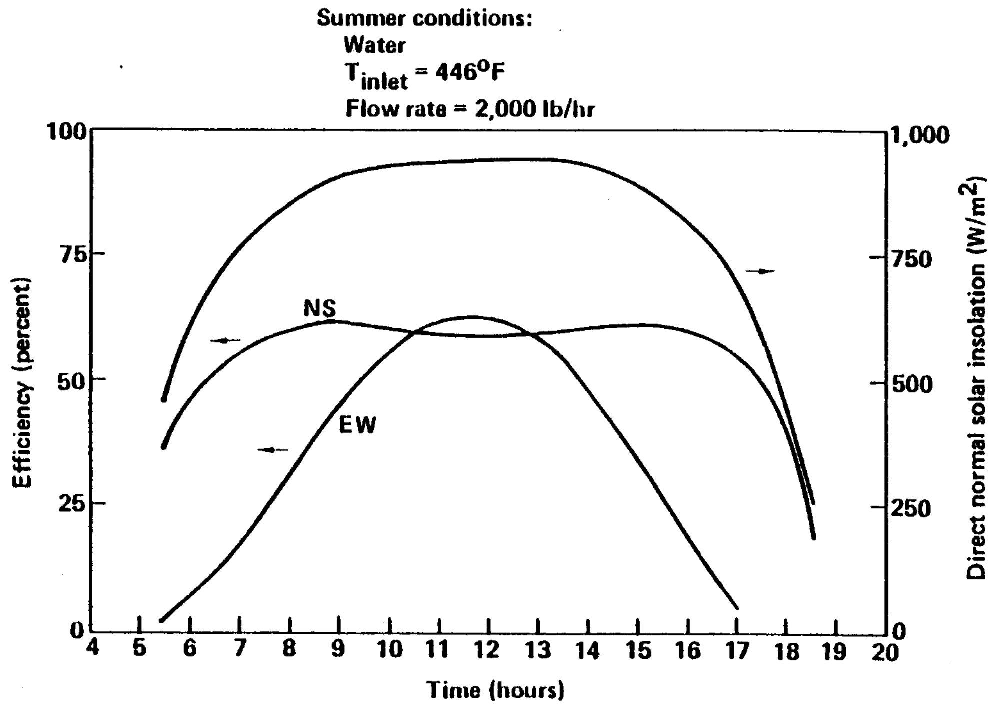

Figure 6-10. Daily Efficiency Profile – Summer

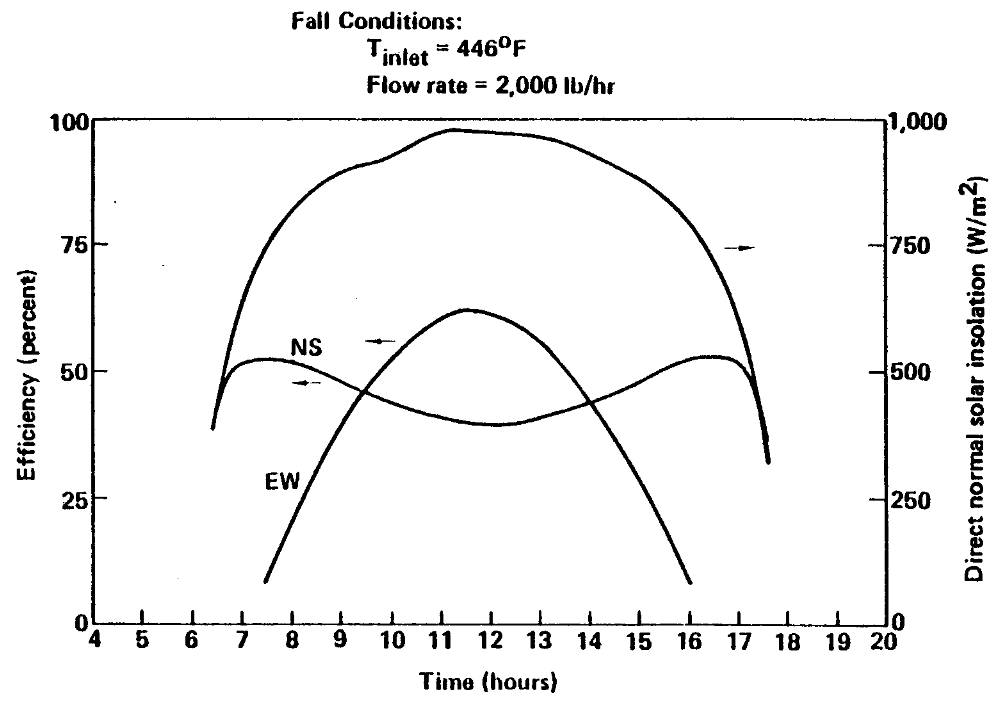

Figure 6-11. Daily Efficiency Profile – Fall

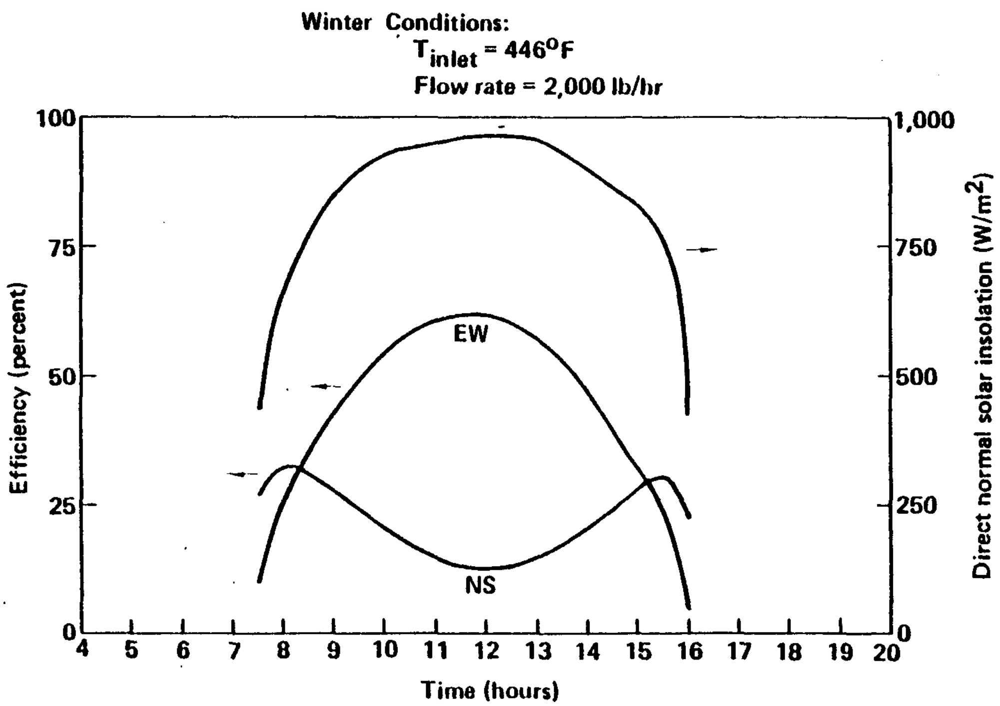

Figure 6-12. Daily Efficiency Profile — Winter

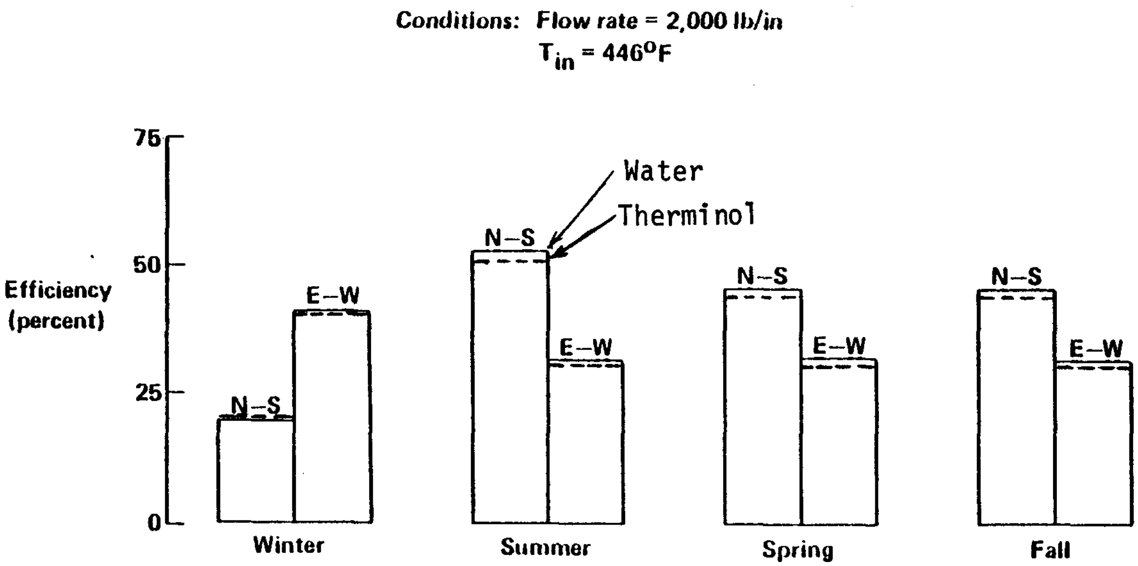

Figure 6-13. Average Daily Efficiencies for Each Season

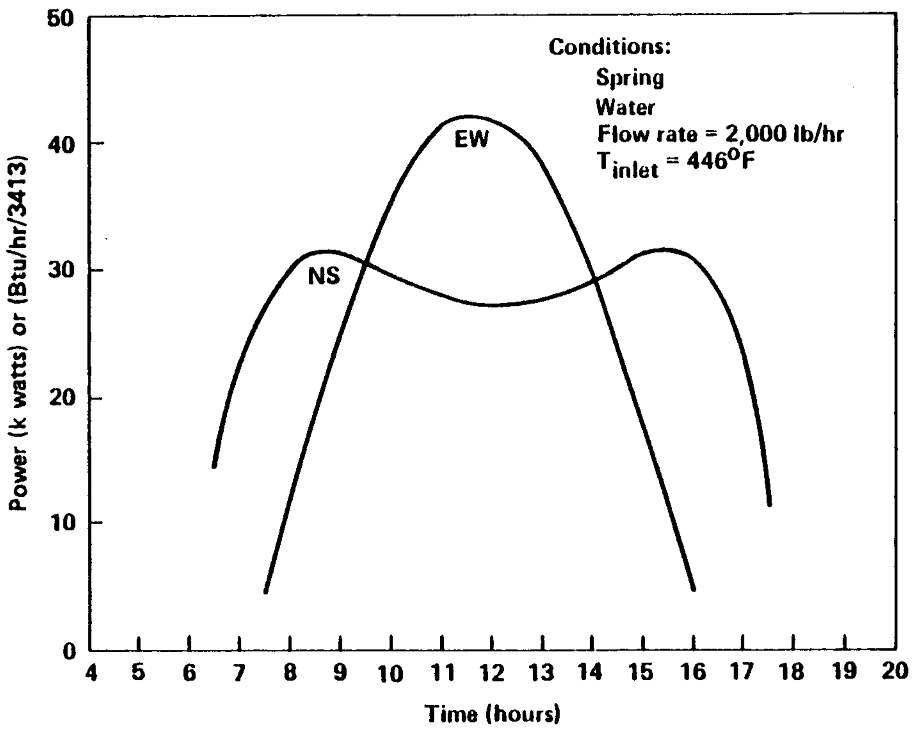

Figure 6-14. Daily Power Production — Spring

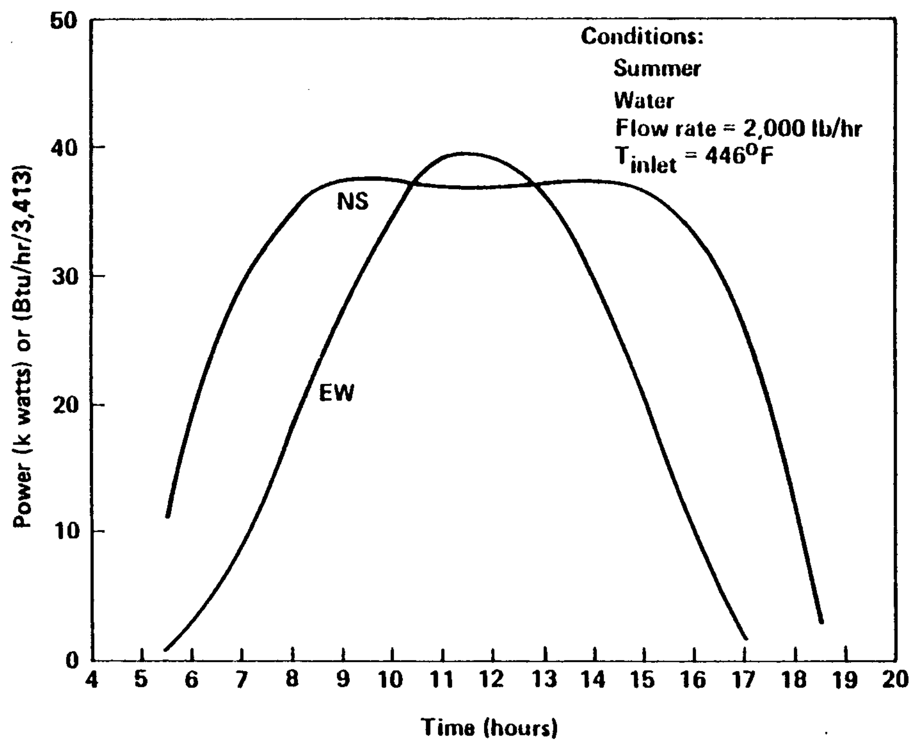

Figure 6-15. Daily Power Production — Summer

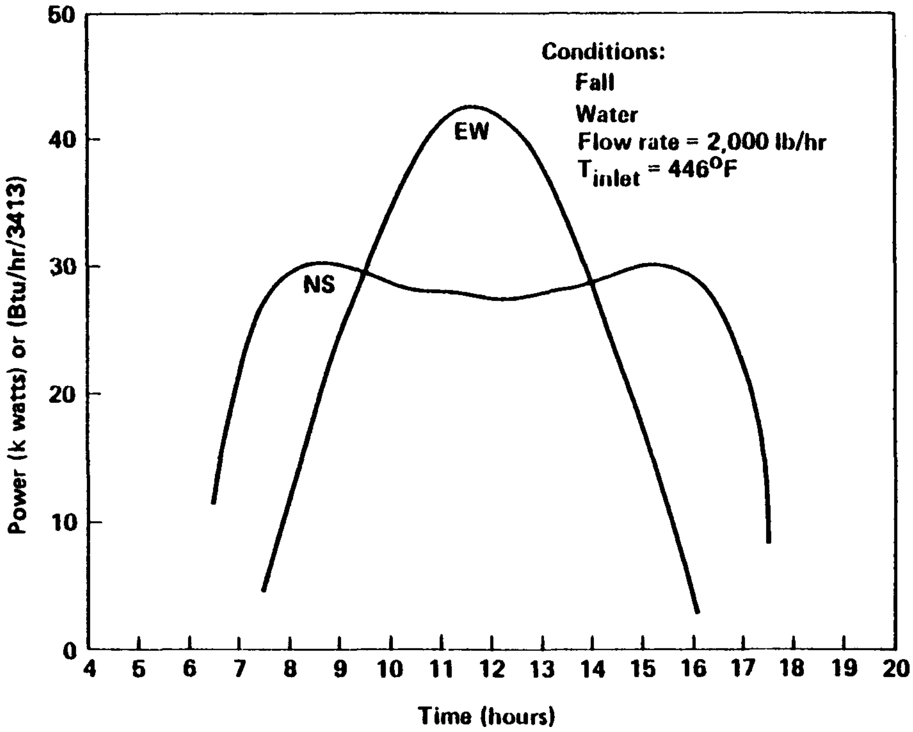

Figure 6-16. Daily Power Production — Fall

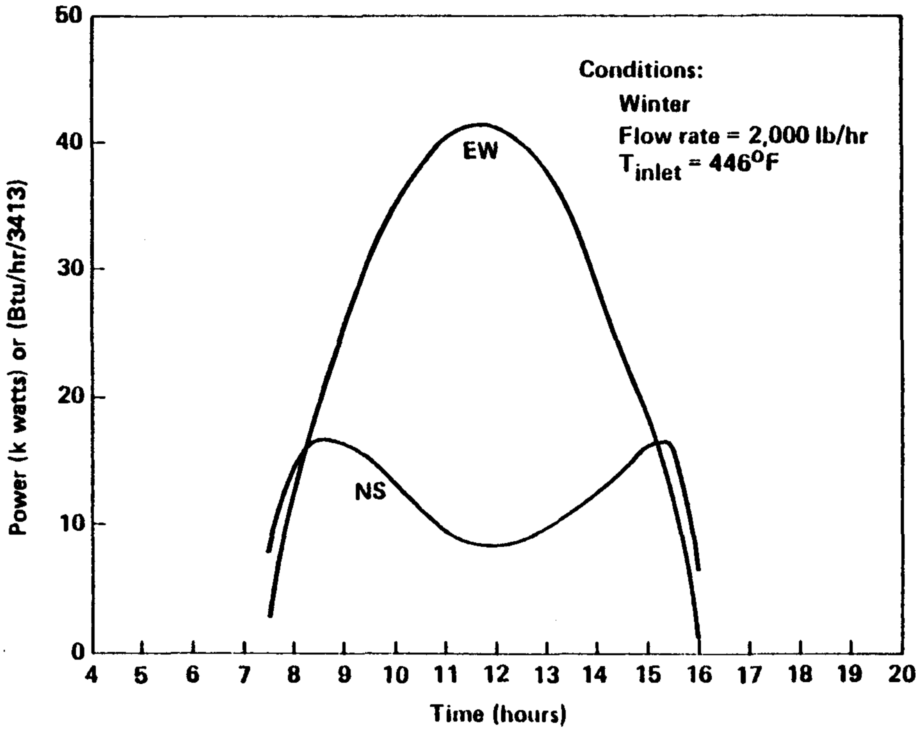

Figure 6-17. Daily Power Production — Winter

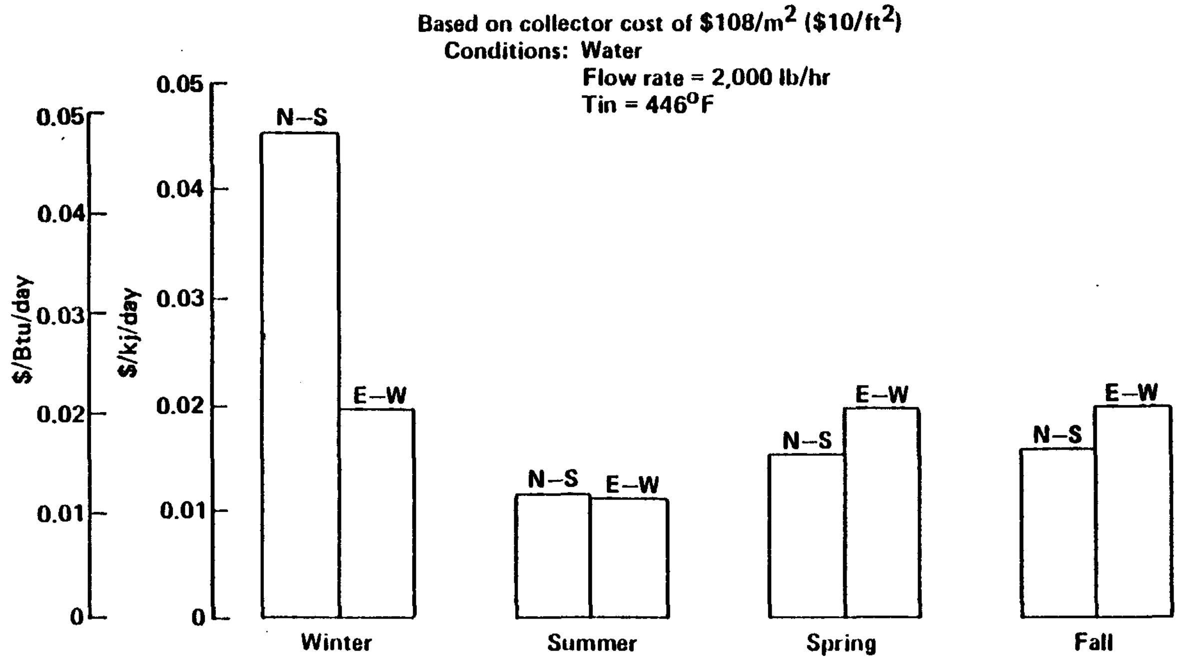

Figure 6-18. Work Figure of Merit for Each Season

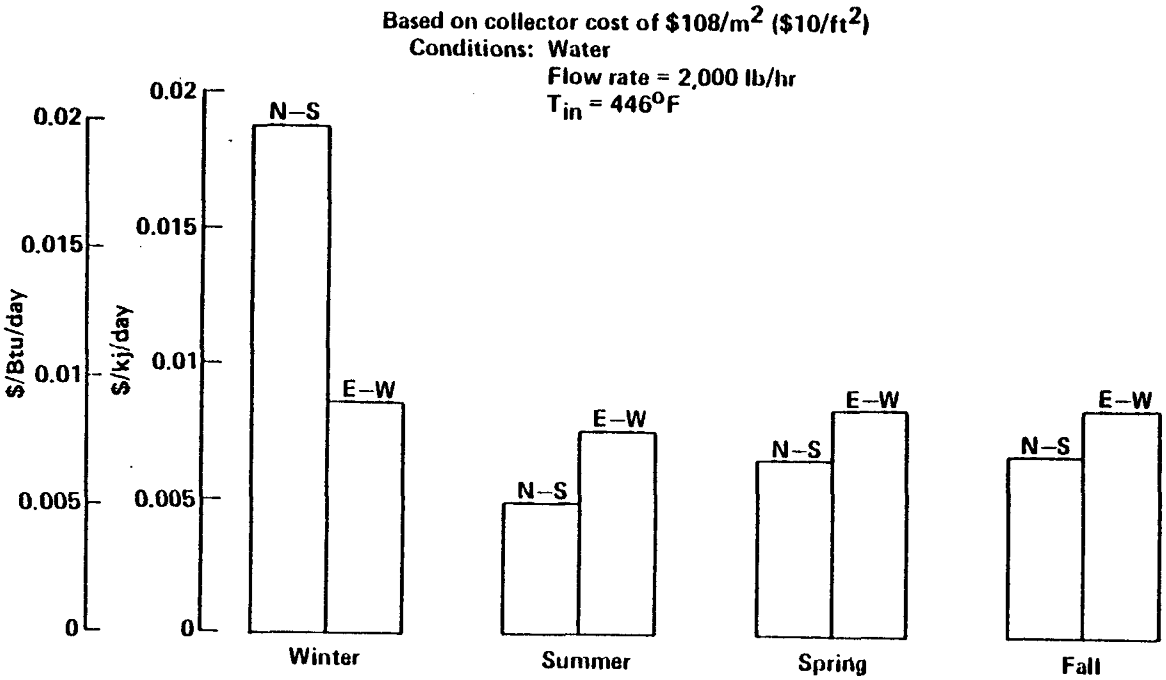

Figure 6-19. Thermal Figure of Merit for Each Season

7.0 MANUFACTURING AND INSTALLATION

7.1 PART FABRICATION

The collector's parts are designed to take advantage of conventional mass production methods such as roll-forming and stamping. From a survey of vendors, it was concluded that a number of qualified cost-conscious suppliers would quote on part fabrication for a production rate of 100,000, m^2 (1,000,000 ft^2) per year. In discussions with fabricators, three areas were recognized as requiring detailed production planning: (1) ring assembly fabrication, (2) enclosure fabrication, and (3) parabolic reflector panels.

While the ring sections themselves are simple roll-formed "hat" sections, there are struts, absorber bearings, gusset plates, and alignment aids that will be attached to form preassembled units that are convenient for installation. Detailed manufacturing planning will be needed to ensure that the predicted low part costs will be attained.

Enclosure fabrication was studied by two vendors: a tent manufacturer and a diversified fabricator of plastic film structures. Budgetary quotes were given based on extrapolation of current polyester film fabrication methods. Each vendor offered innovative concepts for mass production of the film end dome and cylindrical enclosure sections. For example, manufacturing research in automated end dome thermoforming and materials handling and trimming promises to offer lower enclosure parts costs. Of particular concern is maintaining film cleanliness until the product shipped is in dust-proof packaging.

A third area requiring further production planning is the parabolic reflector. Vendor studies have already been performed that indicate, with large quantity production, semi-continuous processing of reflector panels is feasible. Current programs are evaluating alternate reflector manufacturing concepts which appear to offer potential cost savings.

7.2 COLLECTOR ASSEMBLY

Assembly of the collector would initially be in steps as outlined in Table 7-1. This assembly sequence is based on the rings and trusses shipped to the assembly site from vendors as complete assemblies (with struts, rollers, etc.). Assembly would be in a dust-free shop. After assembly, the collectors would be pressurized with dust-free air and transported to a nearby installation site. Some assembly concepts are illustrated in Figures 7-1 and 7-2.

7.3 COLLECTOR INSTALLATION

The collector installation sequence is planned as shown in Table 7-2. An important aspect of the installation plan is that the collectors are received at the site "hermetically sealed" and remain sealed until connected to the central air supply system. This approach requires that "oversize" units be shipped and hoisted (weight is not a problem). For certain installations, it may be worthwhile to trade-off shipping oversize completed collectors versus partial length units that are connected together at the site. Also, situations have been identified where on-site collector assembly is advantageous, providing a dust-free enclosed area is available. A hoisting concept and an installation with an on-site assembly shop is illustrated in Figures 7-3 and 7-4 respectively.

Table 7-1. Collector Assembly Sequence

1. Temporarily secure support trusses to assembly platform.
2. Accurately position the ring assemblies (including absorber support struts and bearings) to the trusses and temporarily fasten to the assembly platform.
3. Install the absorber tube sections and complete bearing assembly.
4. Tighten absorber couplings and end joint flange and seal-weld.
5. Inspect and pressure test absorber joints.
6. Install absorber support cables.
7. Check tension in absorber support cables.
8. Assemble and insert absorber plug sections into absorber tube.
9. Apply sealant strips to ring flanges.
10. Install end dome film sections.
11. Install absorber feed-through insulation parts.
12. Install end dome rotating air seals.
13. Attach thermal protection sensor on absorber.
14. Install outlet end absorber end plumbing parts (flanged elbows, expansion ball joints) and insulation.
15. Install reflectors.
16. Adjust reflector positions (requires special test lamp).
17. Install cylindrical film enclosure sections.
18. Position and tighten film clamps.
19. Install counterweights on rings.
20. Install encoder yoke on end ring.
21. Inflate enclosure with clean, dry air and check for air leaks.
22. Assemble and install drive shaft parts.
23. Install drive cables.
24. Prepare for transportation.

Table 7-2. Collector Installation Sequence

1. Install system heat transfer fluid, cleaning fluid and air supply to header lines.
2. Install the unit controller and motor mount posts.
3. Install gear motor.
4. Set truss anchor bolts.
5. Hoist collectors from transportation rig into final position.
6. Fasten Unit collector to foundation anchor bolts.
7. Connect to fluid and air supply headers.
8. Check tension in drive tables.
9. Install Unit Controller Cabinet.
10. Connect to digital data bus and power lines.
11. Test for air leaks and seal as required.
12. Test all collector functions.
13. Clean Site.

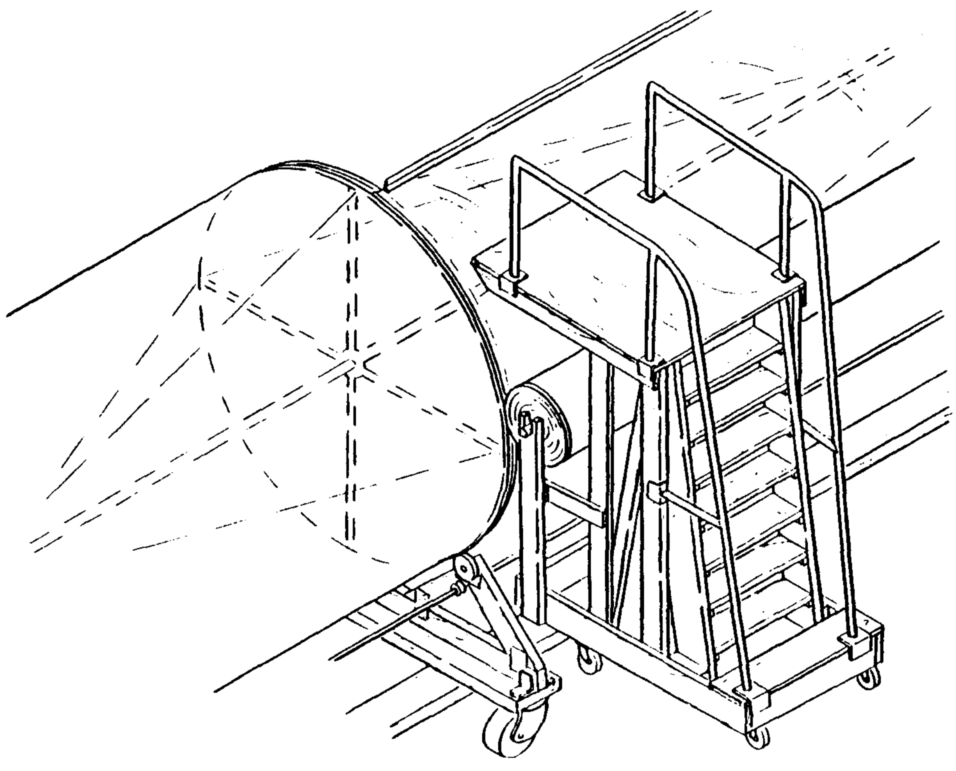

Figure 7-1. Enclosure Installation on Ring Assembly

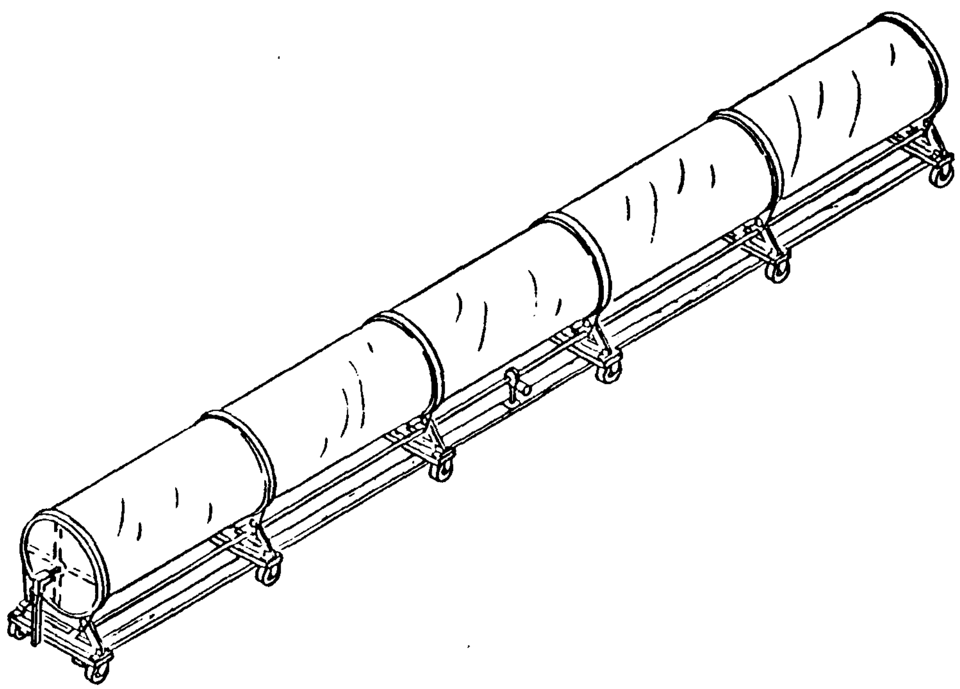

Figure 7-2. Completed Collector on Handling Dolly

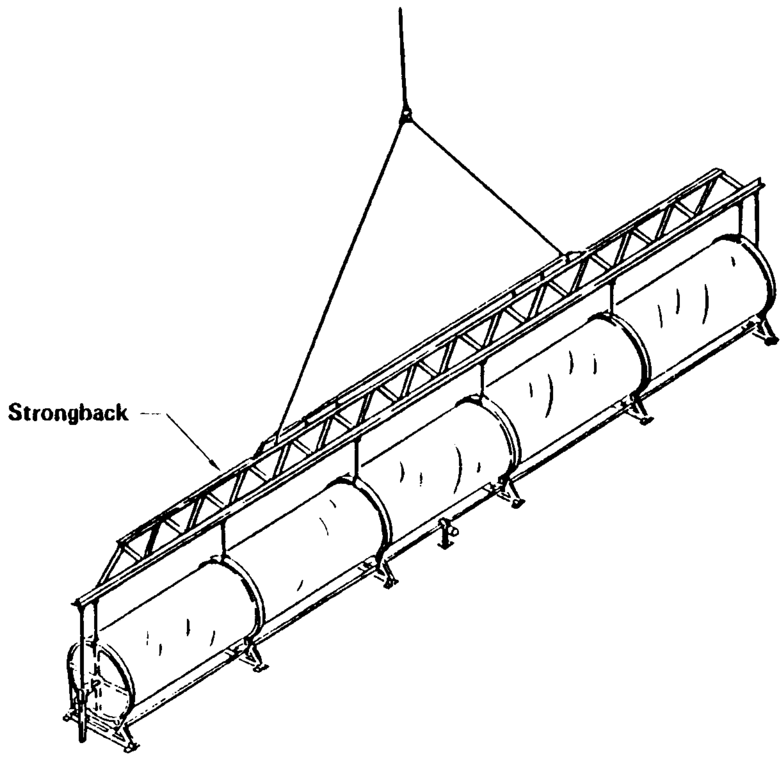

Figure 7-3. Hoisting Method

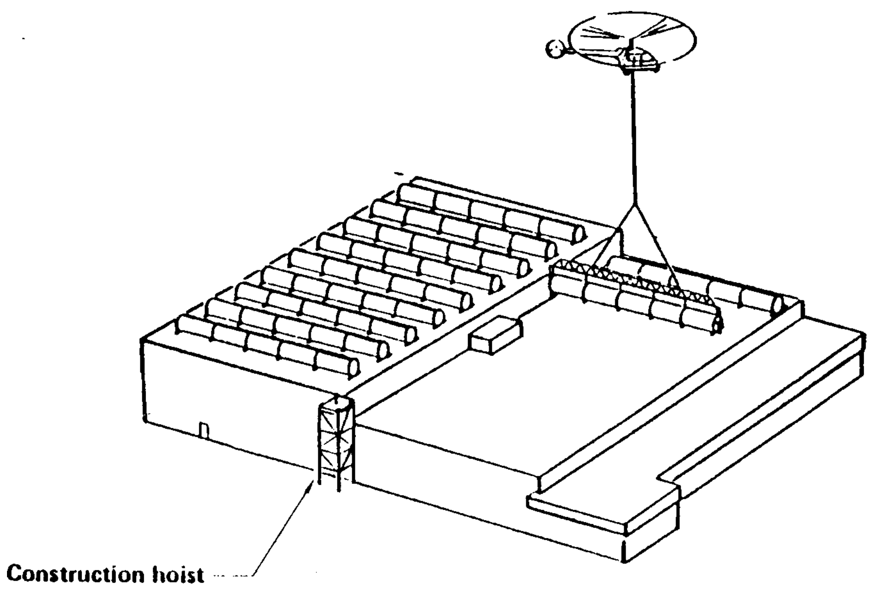

Figure 7-4. Roof Installation by Heliocopter

8.0 MAINTENANCE

8.1 MAINTENANCE REQUIREMENTS

Both routine and unscheduled maintenance of the collectors will be required to assure continuing good performance. The maintenance operations that are envisioned are summarized in Tables 8-1 and 8-2, for the individual collectors and collector field, respectively. The most significant maintenance requirement is associated with enclosure cleaning.

With a gentle cleaning process, as described in Section 8.2, replacement of the film enclosure sections is assumed not to be required over a 20 year life span. However, in case of accidental damage, the film sections can be easily replaced. It is anticipated that field repair kits and temporary sealing covers would be available at a collector site and used to prevent air loss and interior contamination after an accident.

8.2 ENCLOSURE CLEANING

One cleaning concept that is appropriate for the collector is illustrated in Figure 8-1. It consists of a plastic pipe having drilled spray jets which are positioned close to the enclosure. Clean water, with or without detergents would be supplied from a central pressurized source and sprayed by the perforated pipes onto the rotating collector. Waste water would drain down the collector sides and drip into a holding trough below the collectors. The troughs could either be (1) shallow, plastic film lined excavations at a field site, or (2) thin gage galvanized steel pans for a roof top.

The spray pipe would be stored in a safe horizontal position between cleaning periods to avoid shadowing the reflector; the spray jets would

Table 8-1. Collector Maintenance Costs

FUNCTION	SERVICE	REPLACE	REPAIR	FREQUENCY	COSTS: UNIT LABOR HOURS	COSTS: % OF COLLECTOR	COSTS: LABOR HRS PER YEAR	COSTS: MAT'L. $ PER YEAR	COSTS: TOTAL $/YEAR/ COLLECTOR
ENCLOSURE									
Cleaning	X			2 weeks	.0817	100	2.125	9.50	52.00
Patching			X	5 years	1.0	10	0.02	0.80	1.20
Replacement				0					
Joint Sealing	X			5 years	2.0	10	0.04	1.60	2.40
End Dome Seals		X		10 years	4.0	30	0.12	1.6	4.00
Flexible Air Line		X		10 years	.25	50	0.013	.22	0.50
Flow Check Valves				0					
REFLECTOR									
Alignment	X			10 years	12.0	10	0.12	--	2.40
Cleaning				0					
ABSORBER TUBE									
Internal Cleaning				0					
External Cleaning				0					
DRIVE SYSTEM									
Lub. Drive Cables (automatic)	X			4 years	0.125	100	0.031	1.25	1.87
Adjust Cables	X			4 years	1.0	100	0.25	--	5.00
Replace Cables				0					
Drive Shaft Bear.		X		10 years	1.0	100	0.10	1.0	3.00
Gear Motor Brush		X		10 years	1.0	100	0.10	0.5	2.50
Gear Motor Wire	X			10 years	0.25	100	0.025	0.05	0.55
UNIT CONTROLLER									
Encoder Calib.	X			5 years	0.5	100	0.10	--	2.00
Micro-Proc. Bd.		X		10 years	2.0	5	0.07	0.78	0.98
Power Supply	X			10 years	1.0	5	0.005	0.70	0.80
Cabinet Weather-proofing	X			7 years	0.5	100	0.071	0.5	1.92
SUPPORT TRUSSES									
Weather-Proofing	X			7 years	1.5	100	0.22	1.71	6.11
Support Rollers		X		10 years	2.0	25	0.05	0.15	1.15
Total Annual Collector Maintenance Costs									88.38

NOTE: Assumed Labor Rate is $20.00/Hour

Table 8-2. Related System Maintenance Cost

FREQUENCY	SERVICE	REPLACE	REPAIR	FREQUENCY	COST						
					UNIT LABOR HOURS	% OF FIELDS	LABOR HOURS FIELD	LABOR HOURS PER COLLECTOR	MAT'L $/YR/ FIELD	MAT'L $/YR/ COLLECTOR	TOTAL $/YR/ COLLECTOR
<u>SYSTEM CONTROLLER</u>											
Sync. Check	X			Monthly	1.0	100	1.0	0.015	--	--	0.40
Programmable Read-Only Memory Chip (Prom with Solar Ephemeris Data)		X		3 years	2.0	100	2.0	0.030	10.0	0.15	1.00
Micro-Processor Plug-In Board		X		10 years	8.0	10	0.08	0.0012	11.45	0.17	0.19
Back-Up Power Supply	X			Yearly	2.0	100	2.0	0.030	10.0	0.30	0.90
<u>AIR SUPPLY SYSTEM</u>											
Compressor Vane		X		10 years	2.0	100	0.2	0.003	10.0	0.15	0.20
Primary Filter		X		10 years	0.5	100	0.05	0.0007	25.0	0.37	0.39
Secondary Filter				0							
Total											3.08

NOTE: Assumed Labor Rate is $20.00/Hour
67 Collectors/Field

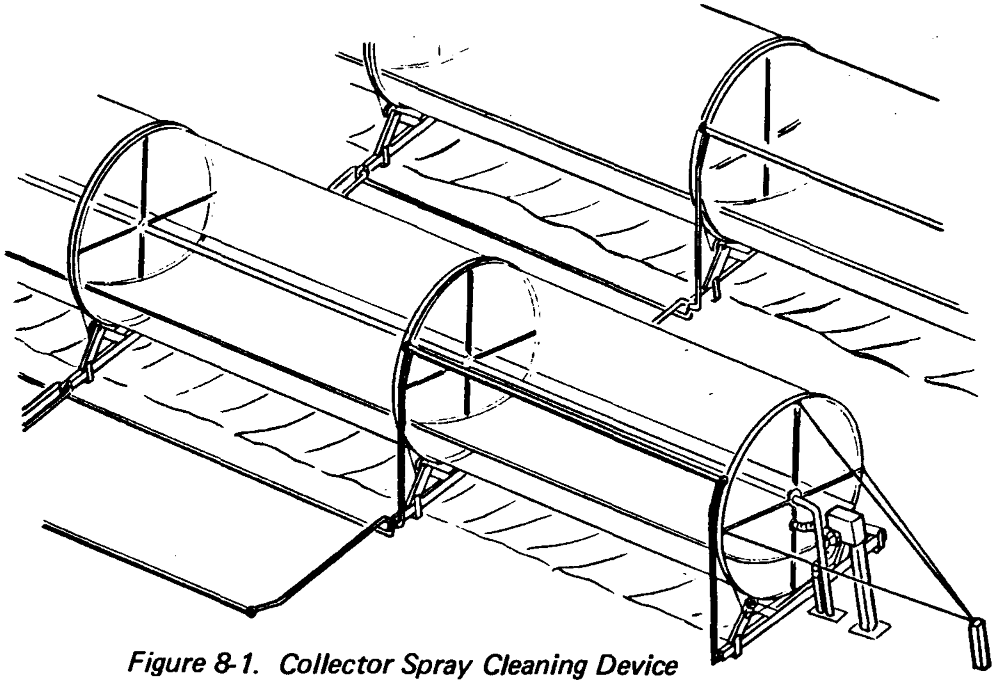

Figure 8-1. Collector Spray Cleaning Device

then be accessible for cleaning if required. Maintenance personnel could quickly erect the spray pipes for a wash and/or rinse cycle. Cleaning would be performed during off-hours while the collectors are being rotated to their part positions by the central system controller.

A representative average rinse frequency is assumed to be once every two weeks. This is a lower frequency than is currently being considered for heliostat fields (Ref. 1), because the collector optical performance is less affected by dust, accumulation, since the light passes through the enclosure once whereas two passes are required for a heliostat.

The interval between rinsing is also increased because of the ability to park the collectors with the window in an essentially vertical position so that rain will have increased rinsing action due to higher run-off velocity. Also, off-hour dust deposition will be predominantly on the collector's upper side. This is important during periods of dew condensation. Dew will preferentially form where water soluble particles are located and on evaporation will leave a salt residue that often has cement-like properties. Based on the above considerations, intervals between low pressure rinsing is expected to be two weeks or longer which should remove most particulate. Once or twice a year rinsing with a high pressure spray should remove the stubborn particulate. Rinsing will also remove particulate held to the enclosure by static forces which can otherwise be a problem with polyester film.

The use of a detergent would not significantly contribute to the cleaning action unless significant hydrocarbon aerosols are present. One concern is that detergents may even be detrimental in presence of ions from certain water soluble particulate types because they may form a tenacious film. Current DOE research in heliostat and collector washing may provide data that can be used to define the above washing requirements more precisely (for example, see Ref. 7).

8.3 CLEANING COSTS

Based on a review of heliostat cleaning estimates (Ref. 1) and discussions at a recent concentrating collector workshop (Ref. 8), cleaning costs are estimated to be as follows for a large collector field having manually erected spray pipes.

Costs per square foot of washed heliostat area discussed at the collector workshop were \$0.00015 for water, \$0.00035 for detergent, \$0.0004 for operation and maintenance, and \$0.003 to \$0.005 for labor. Considering the inherent simplicity of the collector's cleaning concept, a lower labor cost was derived assuming five minutes per collector cycle and a \$20.00 per hour labor rate.

Treated Water	\$0.00025/ft^2
Labor	0.00108
Total Cleaning Cycle Cost	\$0.00133/ft^2 of cleaned area
	\$0.0143/m^2

If half the enclosure's surface area is cleaned, the cleaning cost is \$2.00 per collector (this figure corresponds to the cost data given in Table 8-1).

Hardware and installation costs for the cleaning equipment is estimated to be on the order of \$9.84/m (\$3.00/ft) of collector or \$4.32/m^2 (\$0.40/ft^2) of aperture area.

9.0 COST DATA

9.1 COST ANALYSIS SUMMARY

Estimated costs for the BEC collector are summarized in Table 9-1 for a five year, 500,000 m^2 production run. These costs are based on (1) cost data furnished by various vendors, including those shown in Table 9-2, (2) engineering estimates, and (3) assembly and installation estimates prepared by BOECON, a construction subsidiary of BEC, working with preliminary design drawings. The costs were developed with the following assumptions.

- Five year production run at 100,000 m^2 per year (1428 collectors per year.
- Current materials and processes.
- Current labor rates, fringe benefits, and material costs.
- All parts will be fabricated by vendors who produce commercially oriented commercial products.

Table 9-1. Collector Cost Analysis Summary

ITEM	FIRST YEAR		FIFTH YEAR	
	$/m^2	$/ft^2	$/m^2	$/ft^2
Parts	82.23	7.64	56.40	5.24
Assembly	32.72	3.04	22.50	2.09
Installation:				
Roof Top	42.95	3.99	13.89	1.29
Field	33.80	3.14	10.87	1.01
Total:				
Roof	157.90	14.67	92.79	8.62
Field	148.75	13.82	89.77	8.34

- 69.3 m^2 (746.4 ft^2) Collector
- 100,000 m^2/yr (1,076,390 ft^2) Production Rate
- 85% Learning Curve

Table 9-2. Vendor Study Participants

ITEM	VENDOR	PRODUCT STATUS
Wood Truss Enclosure Supports	Truss-Span, Corp. Redmond, Washington	Special Order
Black Chrome Plated Absorber Pipe	Olympic Solar Plating, Corp., Canton, Ohio	Standard Process
Enclosure Rings	Teledyne Metal Forming Elkhart, Indiana	Special Order
Drive Cables and Fittings	Macwhyte Company Kenosha, Wisconsin	Catalog Items
Enclosure Plastic Film Sections	Space Data Corp. Northfield, Minnesota	Special Order
Parabolic Reflector	Hexcel Corp. Dublin, California	Special Order Using Existing Tooling
Absolute Position Encoder	Litton Industries Chatsworth, California	Model 76
System Controller and Unit Controllers	Cascade Digital Corp. Redmond, Washington	Special Order
Gear Motor and Power Supply	Bodine Company Racine, Wisconsin	Model 42D3BEPM-E
Central Air Compressor	Gast Corp. Benton Harbor, Michigan	Catalog Items

9.2 COLLECTOR PART COSTS

The first year component part costs (summarized in Table 9-1) are compared in relative magnitude in Table 9-3. Significant portions of the part costs are attributed to the parabolic reflector panels, film enclosure and absorber tube assembly. These are portions of the length-dependent costs (like number of cylindrical film sections) that altogether constitute 80 percent of the total part costs.

The part costs were estimated on the basis of the assumed annual production rate using existing materials. Because of the preliminary nature of the design, the vendors were not requested to submit detailed learning curve analyses for part costs. Cost reductions are likely over a five year production run, based on discussions with vendors, so an 85 percent cost improvement curve was applied to arrive at the fifth year part costs. The part costs then are on the order of $4.85/Kg ($2.20/lb) which is a reasonable target for mass produced products. Based on discussions with vendors, promising cost-reducing developments that were assumed to be state-of-the-art in the cost analysis are:

- Availability of polyester films with inherent UV resistance.
- Automated film enclosure production.
- Low-cost parabolic reflector panels produced by continuous processing.

In the electronics area, the unit controller can be implemented using a single chip microcomputer such as Intel's 8748. This device contains, in one package, sufficient program and data storage to perform the function of the unit controller. Only a small amount of interface circuitry (differential live driver and receiver, motor interface circuitry) need be added. Hence, the development cost for the hardware and software will be minimal. In quantity, the unit controller is estimated by a vendor to cost $156.00 at current prices.

The system controller could be implemented using one of the currently available single board computer systems, such as Intel's SBC 80/20. Anticipating a large number of collector installations and a continuing decline in microprocessor component costs, a custom single board computer

Table 9-3. Relative Collector Part Costs

	QUANTITY	TOTAL COST	RELATIVE COST
Cylindrical Film Sections	6	$1,266.00	.222
End Dome	2	177.00	.031
Rings	6	281.00	.049
Film Attachment Band Clamps	12	72.00	.013
Wood Support Truss Assembly	6	131.00	.023
Steel Truss Foundation Frames	6	48.00	.008
Hanger and Tether Cable Assembly	109 m (356 ft)	124.00	.022
Absorber Support Strut Assembly	24	94.00	.016
Parabolic Reflector Panels	81.8 m^2 (880 ft^2)	1,760.00	.309
Absorber Tube Assembly	32.0 m (105 ft)	346.00	.061
Absorber End Fittings and Insulation	2 sets	253.00	.044
Absorber Support Bearings	6	36.00	.006
Air Supply Hose	1	4.00	.001
Counterweight	6	53.00	.009
Gear Motor	1	107.00	.019
Drive Shaft	1	51.00	.009
Encoder	1	110.00	.019
μP Unit Controller	1	156.00	.027
Power Supply	1	70.00	.012
Electronics Cabinet	1	20.00	.004
Digital Data Bus	9.1 m (30 ft)	45.00	.008
Central μP System Cont.	1/50	23.00	.004
Central Air Compressor Filter Unit	1/50	28.00	.005
Miscellaneous Details		179.00	.032
Shipping		271.00	.047
Total		$5,705.00	1.000

will be appropriate for this application. A vendor has estimated that such a board will cost $1145.00 in quantity at current prices.

9.3 ASSEMBLY AND INSTALLATION COSTS

Assembly and installation costs shown previously in Table 9-1 were estimated assuming:

- Collectors will be assembled by a regional franchised assembly shop.
- Completed collectors will be transported 25 miles to the installation site.
- Installation will be accomplished without opening the film enclosure.
- Current labor rates and fringe benefits.
- Typical installation has 67 collectors having an area of 4,645 m^2 (50,000 ft^2).
- 85% cost improvement curve for both shop and site work using a first unit reference value based on the first years average cost.

The assembly shop costs include general conditions, plant, taxes, fee, and bond. Also included are work platforms, equipment, one ton pickups and special transportation trailers. The crew requirements are estimated to be four men plus a 1/3 non-working foreman having an average labor rate of $14.00/hour; the first year production rate is estimated at 56 hours/collector. For the purpose of this study, the entire annual production of 1,000,000 m^2 was assumed at one shop.

Two sites were considered for installation cost comparisons: A roof top in San Antonio, Texas, and a level ground field in Albuquerque, New Mexico. The cost estimates reflect higher costs associated with roof top access problems. The field site was assumed to be level with no rock. Not included are costs that would be common to other comparable collectors or new construction operations such as header piping, power wiring, general conditions and plant materials. The cost estimates include the following installation items.

- Site Layout
- Foundations
- Tether Posts and Cables

- Central Air Compressor/Filter Pack
- Air Supply Lines
- Central Control System
- Digital Data Bus Lines
- Collector Unit Installation
- Unit Controllers
- Drive Motors
- Pressure Testing
- Electrical System Testing
- Site Cleanup

The installation time for both types of sites was estimated at less than 35 days using three four-man crews for collector placement.

10.0 CONCLUSIONS AND RECOMMENDATIONS

The objective of this program was to develop a low cost, innovative preliminary design for a solar collector having good efficiency in heating fluids to the mid-temperature range (outlet temperature greater than 230°C (446°F)). In fulfilling this objective, a preliminary design was developed for a modular, lightweight, linear parabolic trough solar collector which has a pneumatically stabilized, cylindrical clear plastic film enclosure that protects the concentrator and absorber tube. Conclusions from the program are summarized below:

- The collector's cost is projected to be $\$89.74/m^2$ ($\$8.34/ft^2$) of aperture area after a 5 year, 5×10^5 m^2 (5.38×10^6 ft^2) production rim. In terms of cost/performance, the resulting work figure-of-merit ratings for North-South and East-West orientations are 0.0148 and 0.0169 $/kJ/day, respectively (four-season averages). Seasonal work-figure-of-merits for North-South and East range from 0.0101 to 0.040 and 0.0157 to 0.0174, respectively.

- Daily collectors efficiencies in excess of 45% are predicted. For example, an enclosure size of 2.8 m diameter by 30.5 m long (9.33 ft. by 100 ft), an aperture area of 69.3 m^2 (745.9 $ft.^2$), a North-South orientation, and an average sunny spring day in Albuquerque, results in a predicted daily average efficiency of 47%. These conditions yield an energy output of 3.15×10^5 watt-hours for an inlet and outlet water temperature of 230°C (446°F) and 254°C (490°F), respectively; the corresponding mass flow rate is 0.306 liters/sec.(2000 lb./hr.).

- The collector can be operated using either water or organic fluids for the heat transfer fluid.

- The collector's shape and internal pressurization permits wind loads to be carried with an extremely lightweight streamlined structure. This feature cascades throughout the collector unit to result in minimal use of materials.

- The parabolic reflector shell panels are shielded from wind loads, UV radiation and moisture which results in a lightweight reflector having a low cost film reflective surface.
- The reflective surface is protected from the weather, and requires no cleaning. Enviornmental degradation is minimized.
- The convex outside surface of the collector will stay cleaner than an exposed concave mirror surface, thus reducing maintenance costs. Periodic cleaning can be accomplished using simple spray systems.
- The module can be shipped in a compact form and is easily assembled with low installation cost.
- The enclosure can be easily replaced if damaged.
- Since the absorber is in a sheltered environment, satisfactory thermal performance is obtained without convection control devices such as glass covers.
- The stationary feature of the absorber eliminates the need for rotating or flexible fluid couplings and heavy counterweights.
- The inflated enclosure is light and has high torsional stiffness which eliminates the need for heavy force/motion transmission drive lines.
- The lightweight design allows installation on building roofs without major roof modifications.
- The computerized control system provides reliable sun tracking and also functions as an operations controller, warning and data acquisition system. Automatic collector detracking would occur in case of reduced working fluid flow.

To validate the preliminary collector design and predicted performance, detail design, analysis, and production cost studies as well as prototype testing are recommended. As part of the test program, prototype fabrication and manufacturing cost parameters, performance, and methods and frequency of cleaning can be investigated. Important to life-cycle cost is the selection of enclosure film material which will be influenced by the outcome of current vendor development programs. Vendor programs of particular significance are involved with (1) processing biaxially oriented Kynar, an inherently UV stable of airocarbon film, and (2) production of UV stabilized polyester films, having low-cost but shorter life than Kynar.

REFERENCES

1. Solar Central Receiver Prototype Heliostat, Volume 1, Final Technical Report, BEC Document D277-10105-1, Boeing Engineering and Construction, June 1, 1978.

2. Central Receiver Solar Thermal Power System--Collector Subsystem Detail Design Report, BEC Document D277-10022-1, Boeing Engineering and Construction, February 24, 1976.

3. B. O. Almroth, F. A. Brogan and G. M. Stanley, Structural Analysis of General Shells, Volume III, User Instructions for STAGS-C, Lockheed Palo Alto Research Laboratory, December, 1975.

4. ANSYS Engineering Analysis User's Manual, Swanson Analysis Systems, Inc., Elizabeth, Pa., March 1975.

5. R. R. Sowell and R. B. Pettit, Thermal Aging of Electrodeposited Black Chrome, SAND 78-0554, Sandia Laboratories, April, 1978

6. Therminol Fluid Heat Systems Catalog, Monsanto Industrial Chemicals Co., 1978

7. Heliostat Dust Build-up and Cleaning Studies, R. S. Berg, SAND 78-0510, Sandia Laboratories, 1978

8. Solar Thermal Concentrating Collector Technology Symposium, Sponsored by the Solar Energy Research Institute, Denver, Colorado, June 14 and 15, 1978.

9. Suzuki, Sato, Juchi, Yamamoto, Aerodynamic Forces Acting on Circular Cylinders Arranged in a Longitudinal Row, Proceeding of the Third World International Conference on Wind Effects on Buildings and Structures. Tokyo, 1971.

10. J. W. Gerich, An Inflated Cylindrical Solar Concentrator for Producing Industrial Process Heat, Lawrence Livermore Laboratory Report UCID-17612, October 14, 1977.